E-Spectrum Technologies

The University of Texas at Austin
Petroleum and Geosystems Engineering

DOE Project Number DE-FE0024271

Fracture Diagnostics Using Low Frequency Electromagnetic Induction and Electrically Conductive Proppants

PI: Mukul M. Sharma, University of Texas at Austin

Participants: Javid Shiriyev, Peng Zhang, Yaniv Brick, Ali Yilmaz, UT Austin.

J. Gabelmann, Robert Houston, ESTI

August 2, 2017

Objectives

- To build and test a downhole fracture diagnostic tool that can be used to estimate the orientation and length of the 'propped' fracture (not the created fracture)
- To map the distribution of proppant in the fracture.

Technical Approach

- The project has the following components:
  - Develop a forward model for the proposed EM technology taking into account real geological and reservoir constraints.
  - Source and test proppants in the laboratory for electrical and material properties for their suitability in deployment in the field.
  - Design, build and field test a low frequency electromagnetic tool.
  - Invert the field data to estimate the propped fracture geometry, and present a stimulated rock volume map.

Project Tasks

- Task 1.0 - Project Management Plan
- Task 2.0 - Development of forward model using proposed tool and different fracture geometries
- Task 3.0 - Lab testing of selected proppants for electrical and material properties
- Task 4.0 – Design and construction of a low frequency electromagnetic tool
- Task 5.0 – Laboratory and testing of tool in a shallow test site.
- Task 6.0 - Inverting the field data to obtain the fracture geometry

E-Spectrum Technologies

The University of Texas at Austin
Petroleum and Geosystems Engineering

Electrically Conductive Proppant Resistivity and Permeability Lab Measurements

Peng Zhang

Rod Russel

Williams Ozowe

Mukul Sharma

E-Spectrum Technologies

The University of Texas at Austin
Petroleum and Geosystems Engineering

Experimental Method for Resistivity Measurements

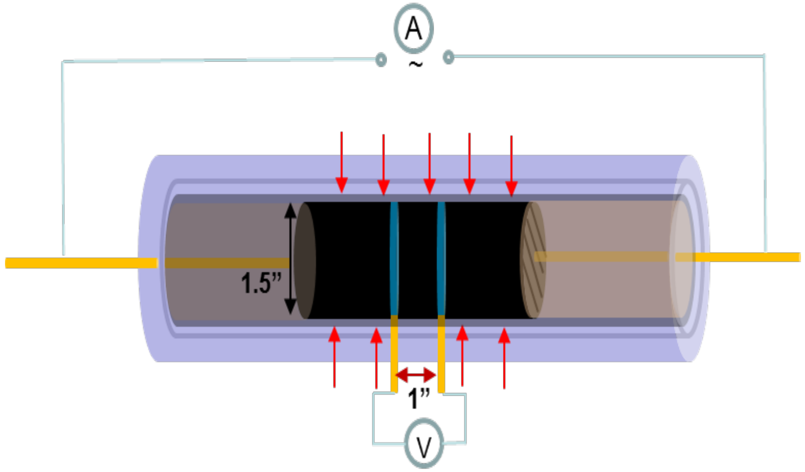

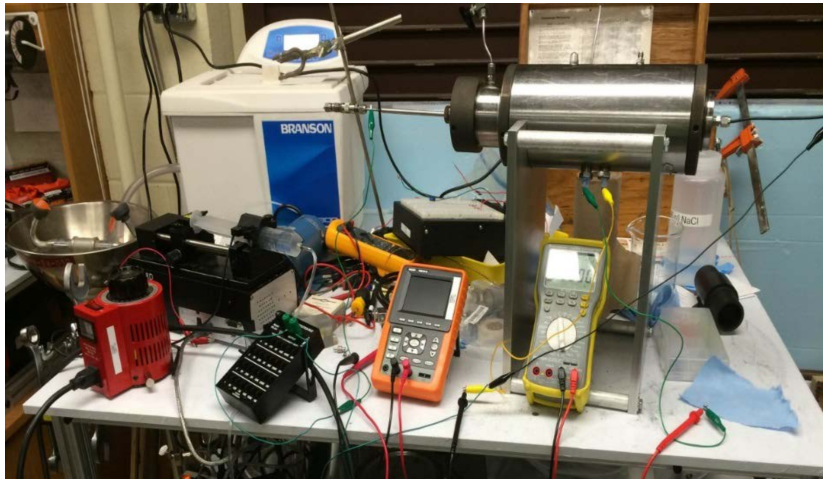

- A **4-electrode method** was used to do the measurements in a core holder.
- Alternating current **(AC)** was applied on the current-carrying electrodes, while the voltage was measured on the voltage-sensing electrodes.
- **Confining pressure** can be applied. Saturation fluid could be tuned.

Experimental Method for Resistivity Measurements

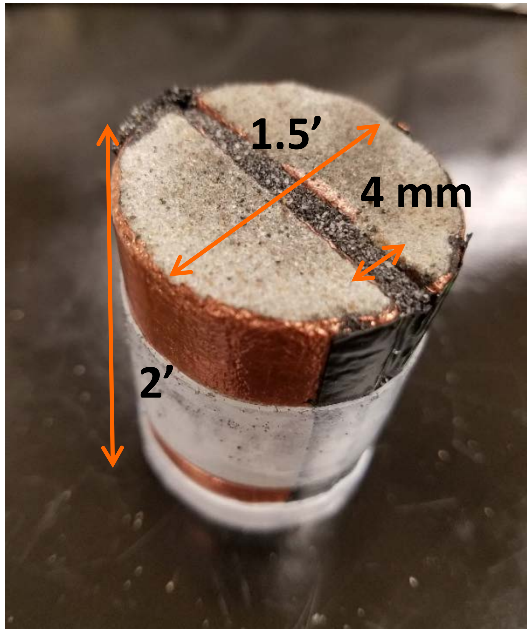

Before measurement

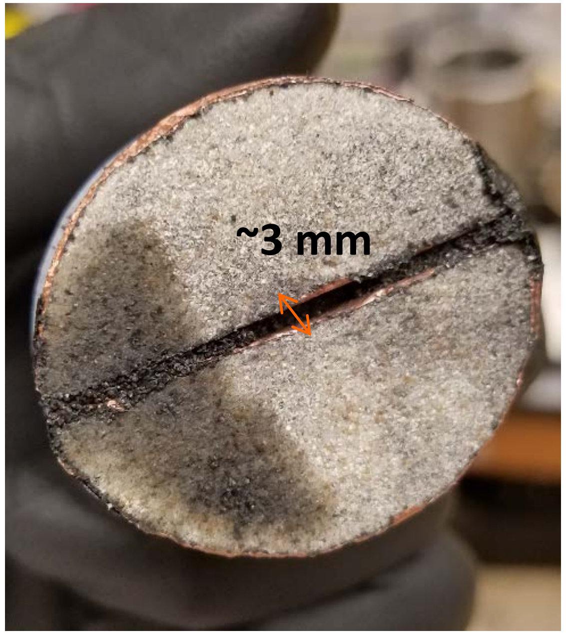

After measurement

- 0% sand + 100% coke
- 25% sand + 75% coke
- 50% sand + 50% coke
- 75% sand + 25% coke

The ratio is based on **mass.**

Size:40-70 mesh & 70-100 mesh
Coke Density: ~2 g/cm^3

Electrical Resistivity: 40/70 mesh

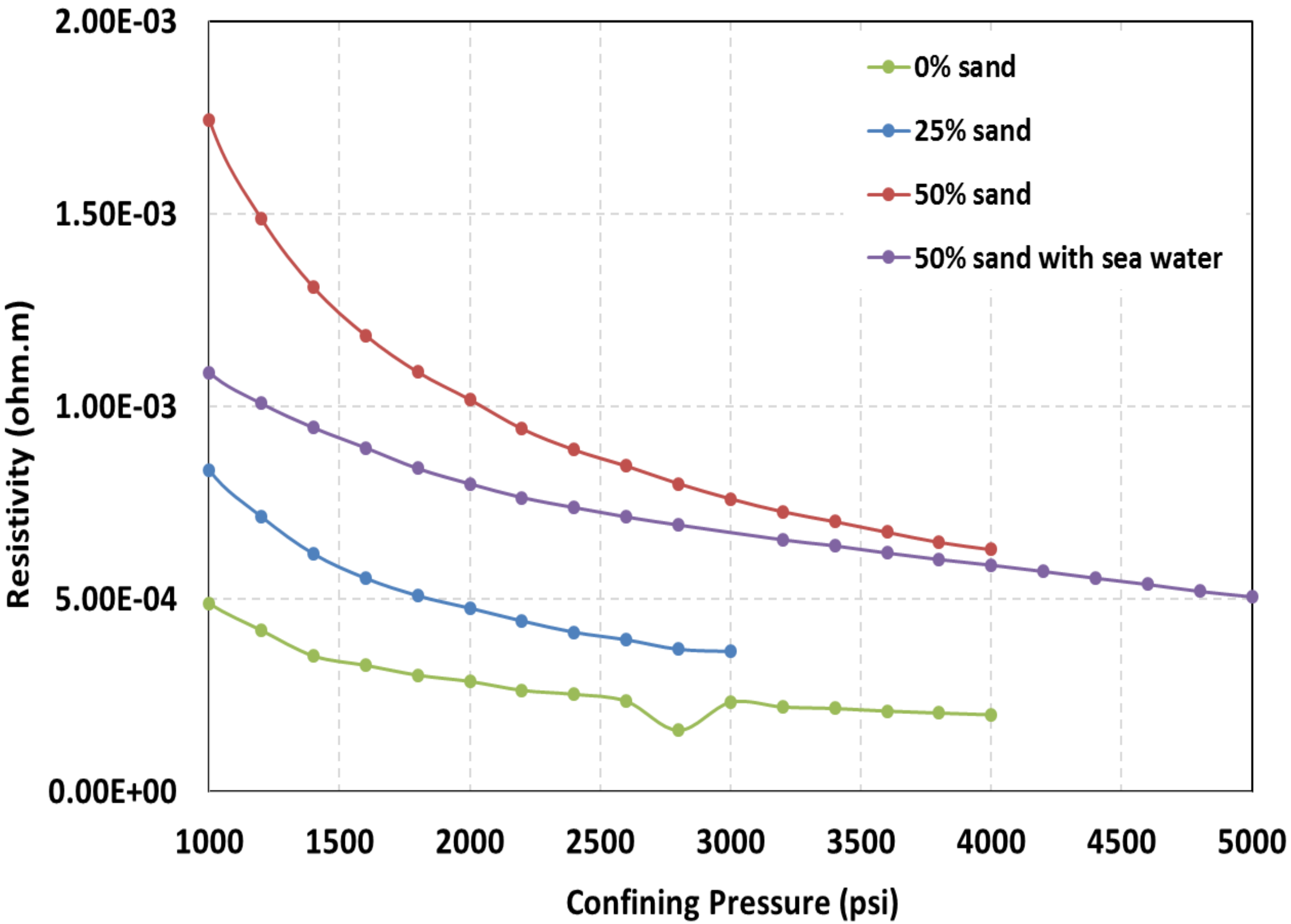

0% sand	$1.99 \times 10^{-4}\ \Omega \cdot m$ @4000 psi
25% sand	$3.64 \times 10^{-4}\ \Omega \cdot m$ @3000 psi
50% sand	$6.28 \times 10^{-4}\ \Omega \cdot m$ @4000 psi
50% sand (sea water)	$5.06 \times 10^{-4}\ \Omega \cdot m$ @5000 psi

Electrical Resistivity: 70/100 mesh

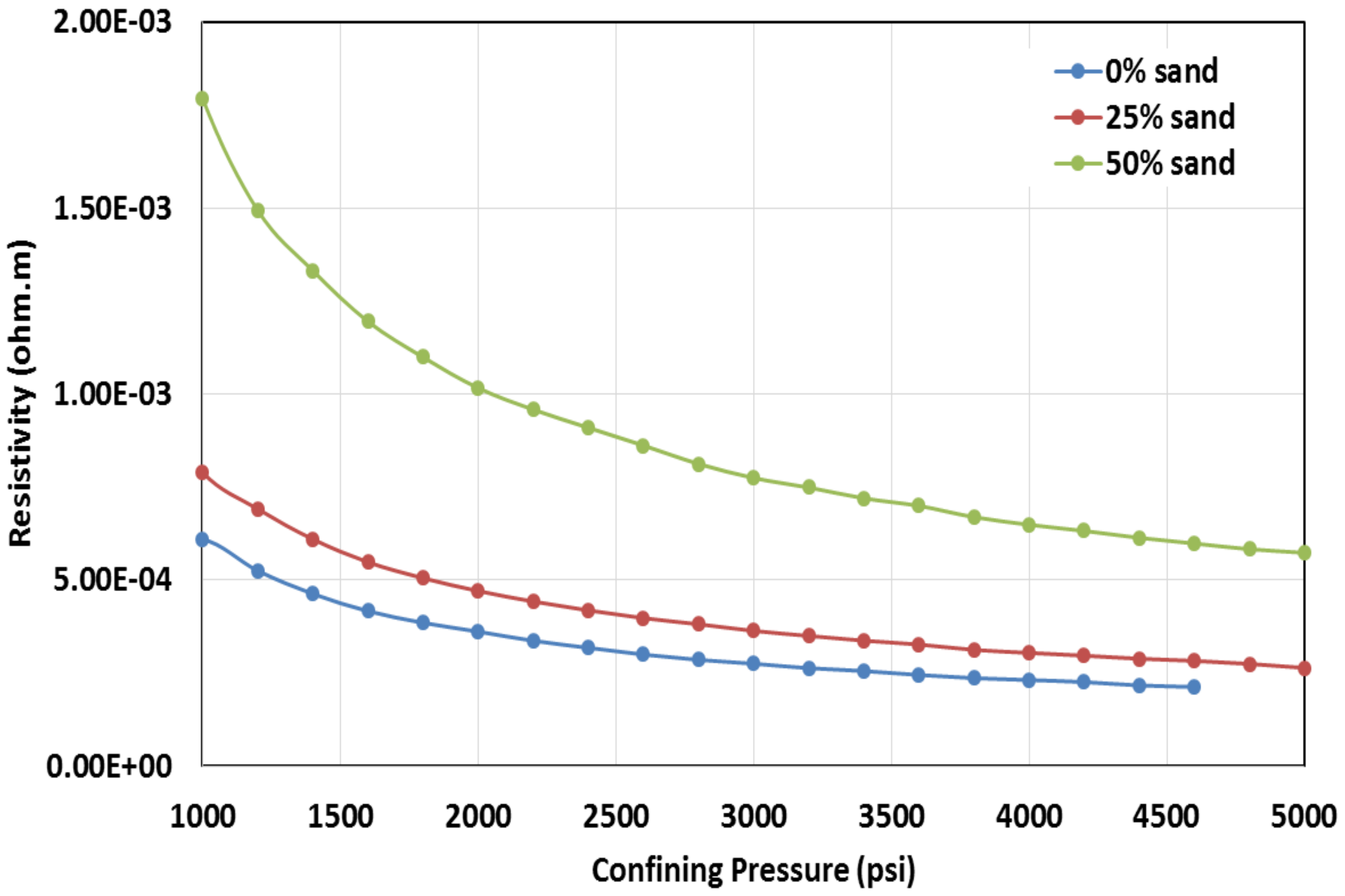

All with sea water

0% sand	$2.12 \times 10^{-4}\ \Omega \cdot m$ @4600 psi
25% sand	$2.64 \times 10^{-4}\ \Omega \cdot m$ @5000 psi
50% sand	$5.73 \times 10^{-4}\ \Omega \cdot m$ @5000 psi

Electrical Resistivity: 70/100 mesh

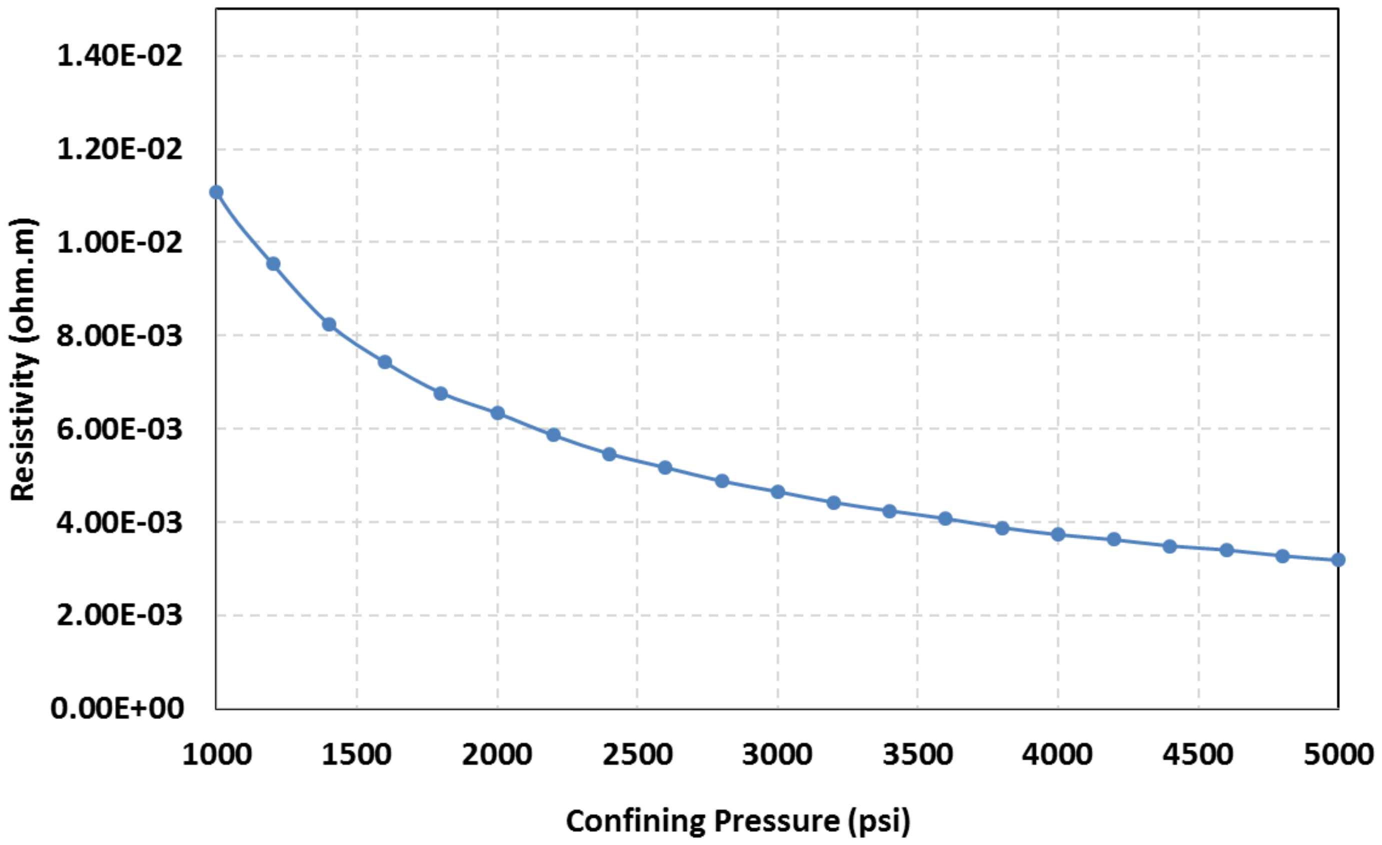

75% sand (sea water)	$3.18 \times 10^{-3}\ \Omega \cdot m$ @5000 psi

Experimental Method for Fracture Conductivity Measurements

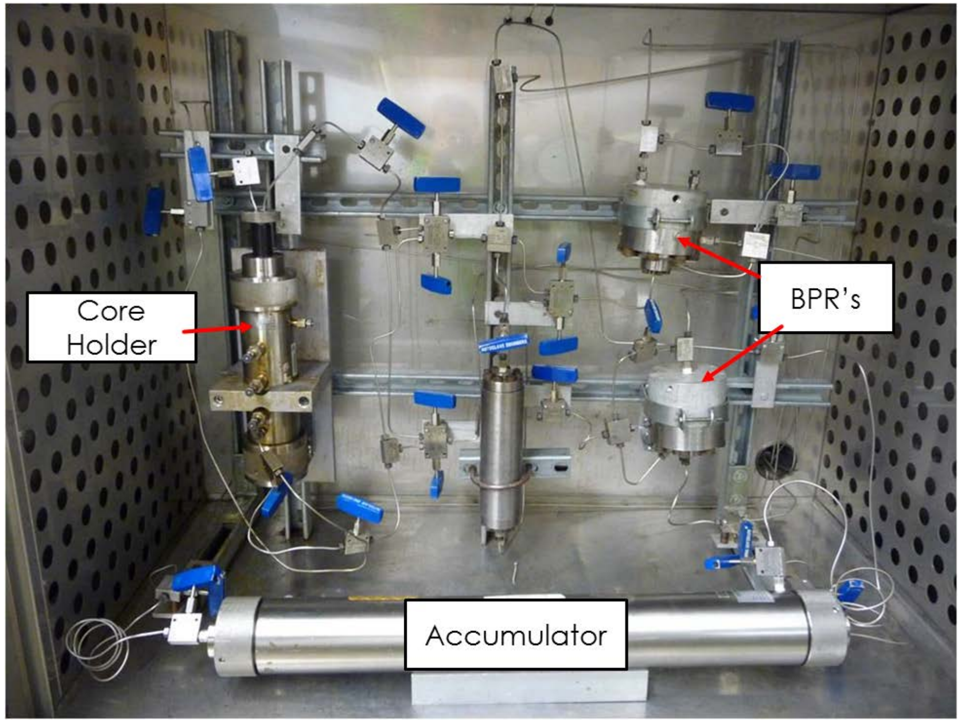

- A Berea sandstone core of 1'' diameter by 8'' length was prepared with a fracture width of 1mm.
- The core was placed inside a Hassler sleeve core holder and **evacuated** to remove trapped air.
- Confining closure stress was applied for 24 hours, after which 3% brine solution was pumped through the core at a range of **constant flow rates**.
- For each closure stress applied, the **pressure drop** across the core was measured and used to calculate the fracture conductivity using Darcy's Law.
- This procedure was repeated for incremental closure stresses from 1000 – 8000 psi.

E-Spectrum Technologies

The University of Texas at Austin
Petroleum and Geosystems Engineering

Fracture Conductivity and Normalized Conductivity
Sand vs Coke: 40/70 mesh

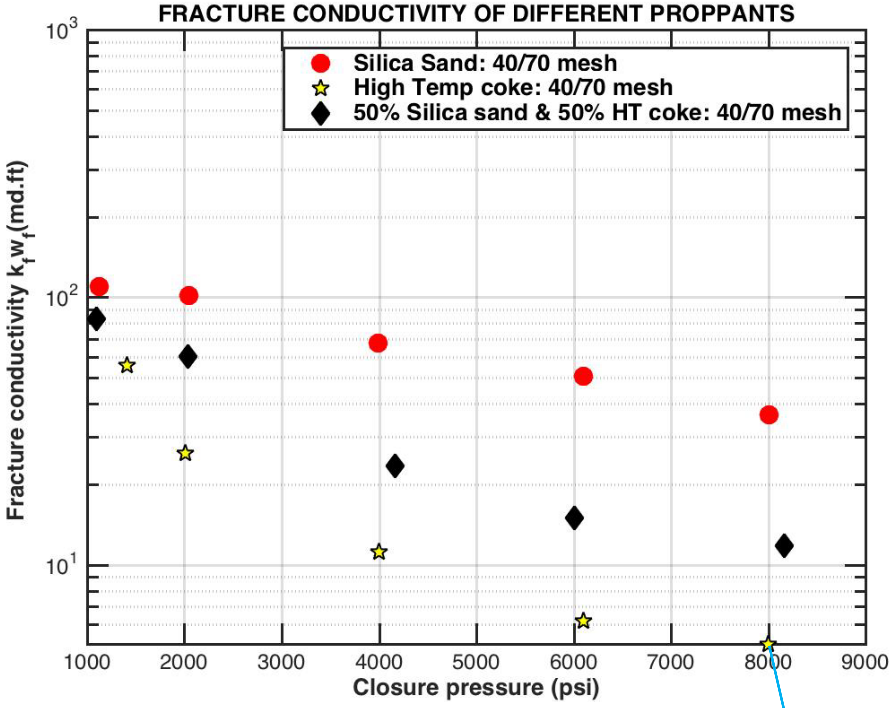

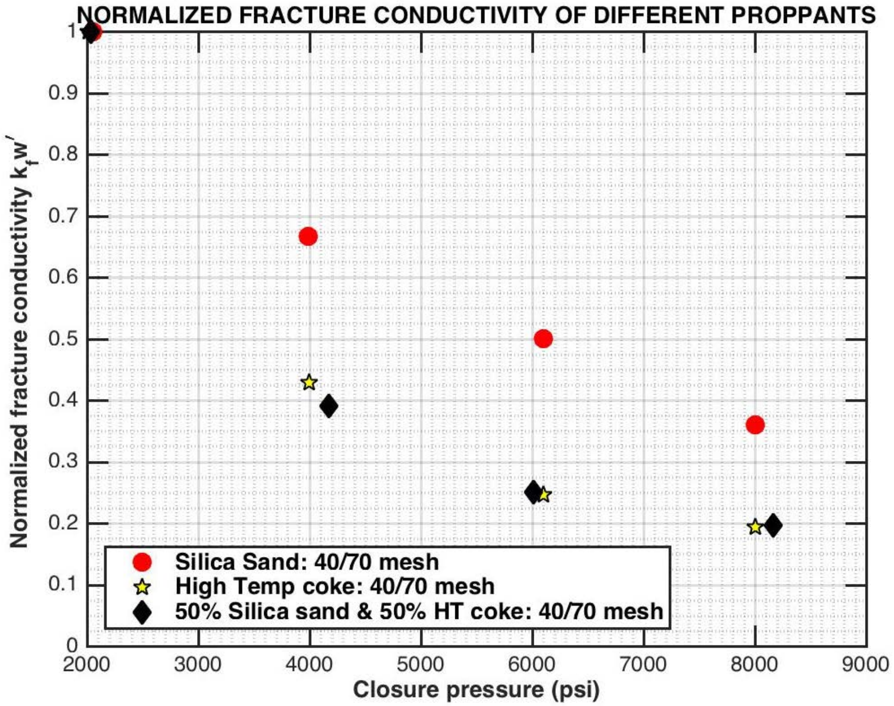

$F_{CD} = k_f * w / L_f * k$

$F_{CD} = 5 / (250*10^{-4})$

$F_{CD} = 200$

Productivity Index: Fractured Vertical Wells

Ref: Friehauf and Sharma (2009)

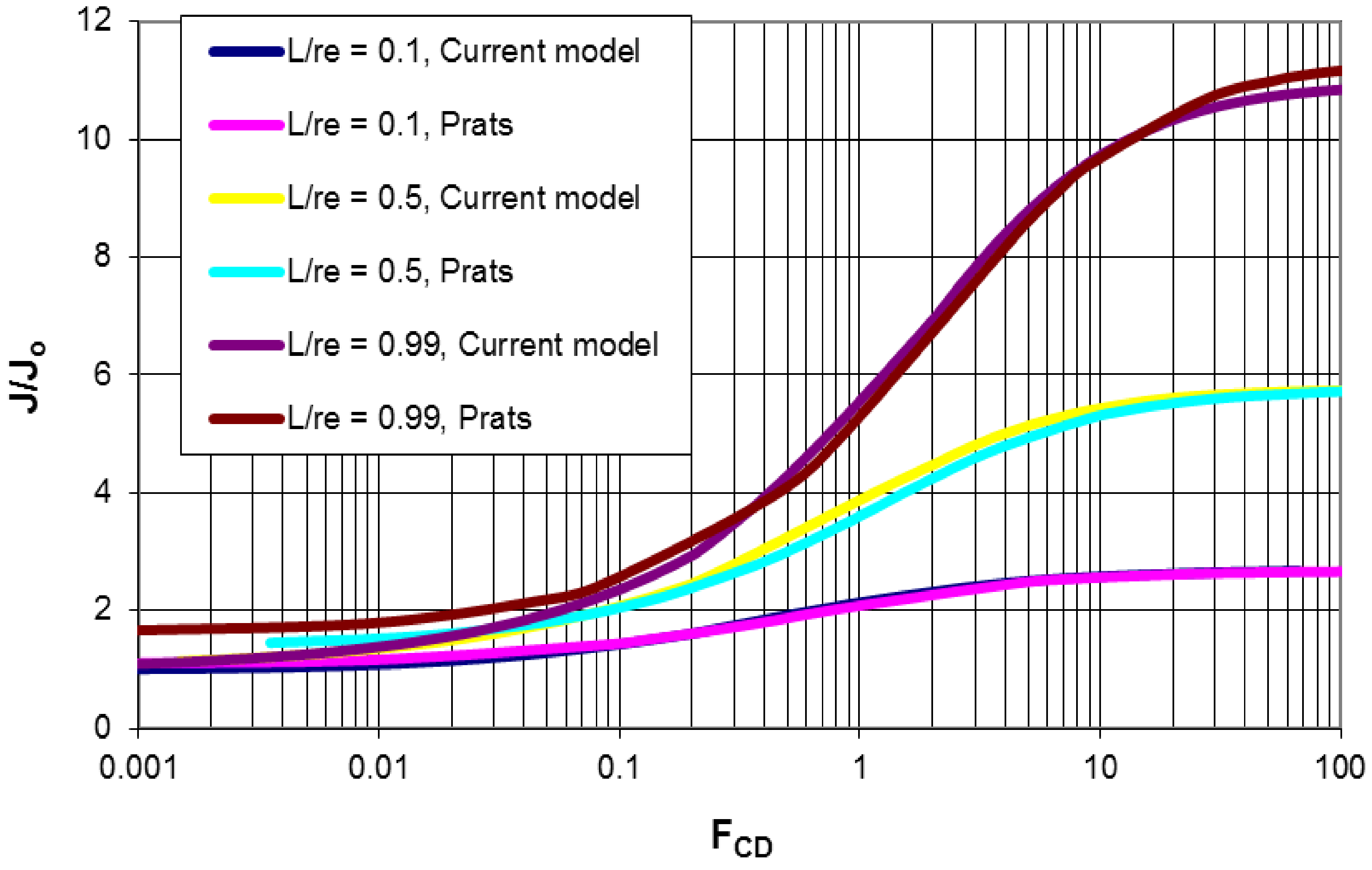

Fracture Conductivity and Normalized Conductivity

Sand vs Coke **70/100 mesh**

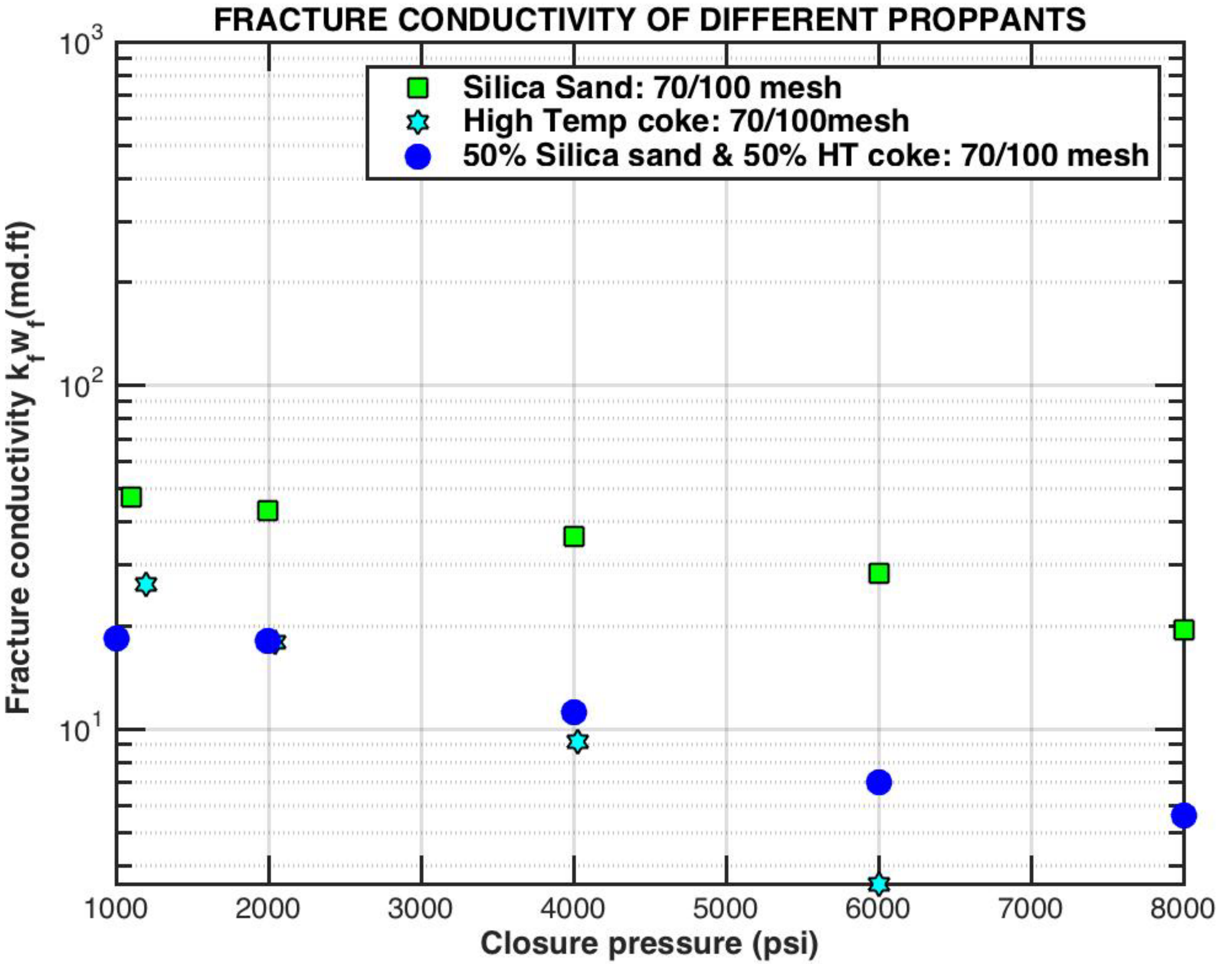

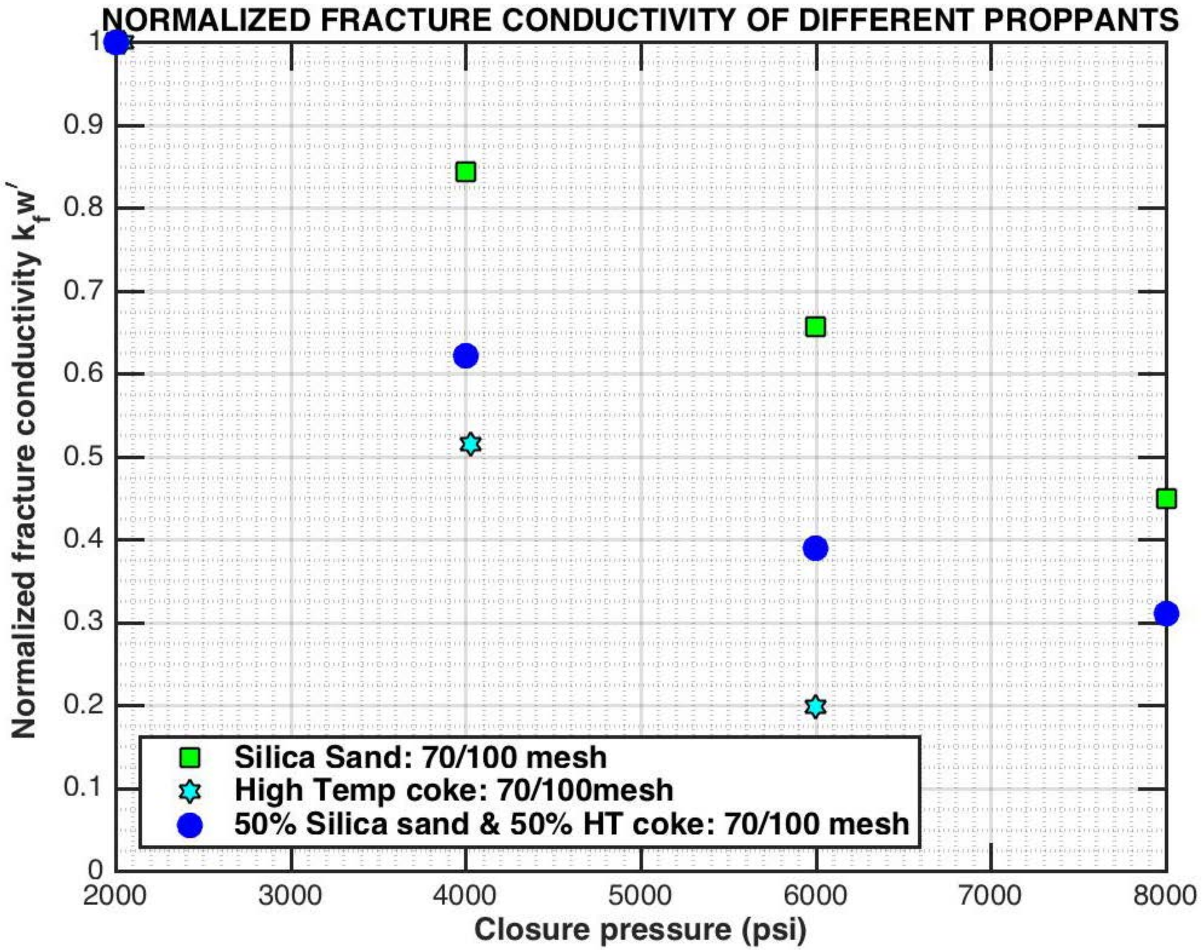

Summary of Lab Measurements

- The electric resistivity of the PC, under confining stress, was measured to be in the range of 2 x 10^{-4} $\Omega \cdot m$
- Size does not affect the electrical resistivity but does affect the permeability.
- It is feasible to use mixtures of sand and PC if fracture conductivity is a concern (large in-situ stresses).
- Both resistivity and permeability increase with increasing mass percentage of sand at a given confining pressure.
- Brine has a minor effect on the measured resistivity because it is usually much more resistive ($\sim 0.2\ \Omega \cdot m$) than petroleum coke.

Tasks

- Task 1.0 -- Project Management Plan
- Task 2.0 - Development of forward model using proposed tool and different fracture geometries
- Task 3.0 - Lab testing of available proppants in the market for electrical and material properties
- Task 4.0 – Final design and construction of low frequency electromagnetic tool
- Task 5.0 – Laboratory and field testing of tool
- Task 6.0 -- Inverting the field data to obtain the fracture geometry

Numerical Simulation

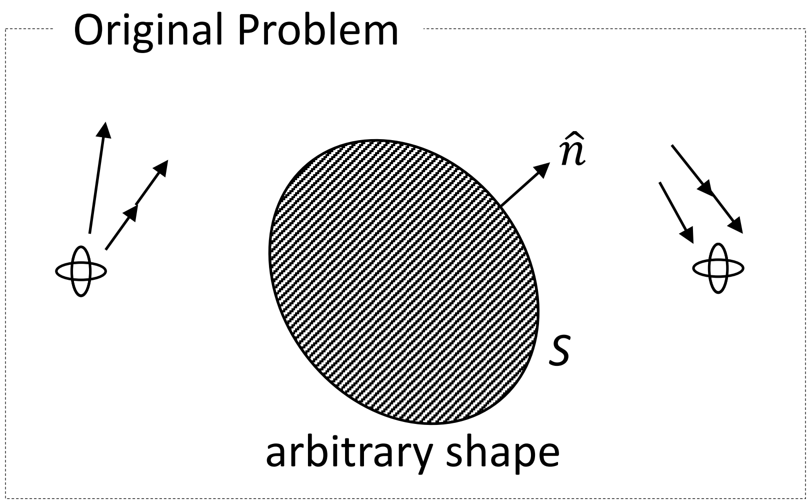

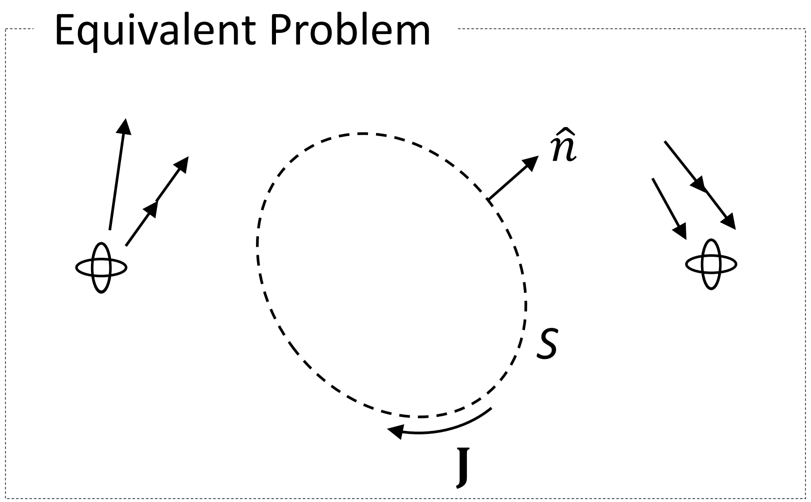

Maxwell Equations:

$$\nabla \times \mathbf{E} = -j\omega\mu\mathbf{H} - \mathbf{M}$$
$$\nabla \times \mathbf{H} = j\omega\varepsilon\mathbf{E} + \mathbf{J}$$
$$\nabla \cdot (\varepsilon\mathbf{E}) = \rho_e$$
$$\nabla \cdot (\mu\mathbf{H}) = \rho_m$$

$$\mathbf{E}^{\text{sca}} = -j\omega\mu \iint_S G(\mathbf{r},\mathbf{r}')\mathbf{J}(\mathbf{r}') + \frac{\nabla G(\mathbf{r},\mathbf{r}')}{k^2}\nabla' \cdot \mathbf{J}(\mathbf{r}')\, dS'$$

$$\mathbf{H}^{\text{sca}} = \iint_S \nabla G(\mathbf{r},\mathbf{r}') \times \mathbf{J}(\mathbf{r}')\, dS'$$

Numerical Simulations

* Simplest coil model
* reference: current source

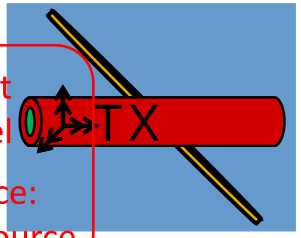

$\equiv$

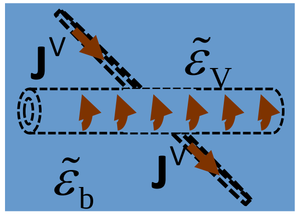

$$\tilde{\varepsilon}_{\mathrm{V}}(\mathbf{r}) = \varepsilon_{\mathrm{V}}(\mathbf{r}) + \sigma_{\mathrm{V}}(\mathbf{r})/j\omega$$

$$\mathbf{J}^{\mathrm{V}}(\mathbf{r}) = \underbrace{\left(1 - \frac{\tilde{\varepsilon}_{\mathrm{b}}}{\tilde{\varepsilon}_{\mathrm{V}}(\mathbf{r})}\right)}_{\chi(\mathbf{r})} j\omega\tilde{\mathbf{D}}(\mathbf{r})$$

$$0 < |\chi| < 1$$

$$\tilde{\mathbf{D}}(\mathbf{r}) = \tilde{\varepsilon}_{\mathrm{V}}(\mathbf{r})\mathbf{E}(\mathbf{r}) \qquad \forall \mathbf{r} \in V$$

$$\frac{\tilde{\mathbf{D}}(\mathbf{r})}{\tilde{\varepsilon}_{\mathrm{V}}(\mathbf{r})} + \mathrm{L}\left(j\omega\chi\tilde{\mathbf{D}},\mathbf{r}\right) = \mathbf{E}^{\mathrm{inc}}(\mathbf{r})$$

Electric-field integral-equation

$$\mathrm{L}(\mathbf{J}^{\mathrm{v}},\mathbf{r}) = j\omega\iiint_V \mu_0 G(\mathbf{r},\mathbf{r}')\mathbf{J}^{\mathrm{v}}(\mathbf{r}')dv' - \nabla\iiint_V G(\mathbf{r},\mathbf{r}')\frac{\nabla'\cdot\mathbf{J}^{\mathrm{v}}(\mathbf{r}')}{j\omega\tilde{\varepsilon}_{\mathrm{b}}}dv'$$

$$G(\mathbf{r},\mathbf{r}') = \frac{e^{-\gamma_{\mathrm{b}}|\mathbf{r}-\mathbf{r}'|}}{4\pi|\mathbf{r}-\mathbf{r}'|}, \ \gamma_{\mathrm{b}} = j\omega\sqrt{\mu_0\tilde{\varepsilon}_{\mathrm{b}}}$$

- Discretize geometry expand unknowns

$$\tilde{\mathbf{D}}(\mathbf{r}) \cong \sum_{k'=1}^{N}\mathbf{I}[k']\mathbf{f}_{k'}(\mathbf{r})$$

$$\frac{\mathbf{J}^{\mathrm{V}}(\mathbf{r})}{j\omega} \cong \sum_{k'=1}^{N}\chi_{k'}(\mathbf{r})\mathbf{I}[k']\mathbf{f}_{k'}(\mathbf{r})$$

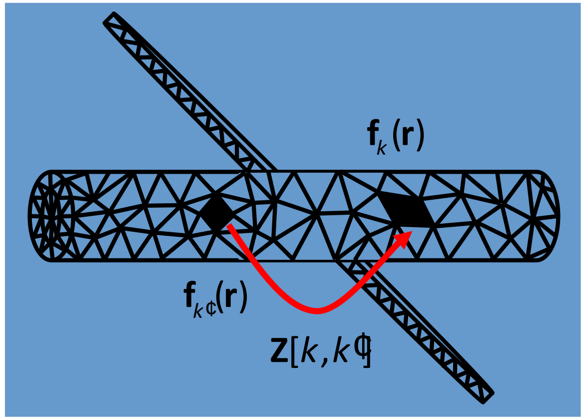

- Galerkin testing

$$\left\langle \chi_k(\mathbf{r})\mathbf{f}_k(\mathbf{r}), \frac{\tilde{\mathbf{D}}(\mathbf{r})}{\tilde{\varepsilon}_{\mathrm{V}}(\mathbf{r})} + \mathrm{L}(j\omega\chi\tilde{\mathbf{D}},\mathbf{r})\right\rangle = \left\langle \chi_k(\mathbf{r})\mathbf{f}_k(\mathbf{r}), \mathbf{E}^{\mathrm{inc}}(\mathbf{r})\right\rangle$$

- System of linear equations $\mathbf{Z}_{N\times N}\mathbf{I}_{N\times 1} = \mathbf{V}^{\mathrm{inc}}_{N\times 1}$

- Multiple tool positions $\mathbf{Z}[\mathbf{I}_1 \cdots \mathbf{I}_{N_{\mathrm{rhs}}}] = [\mathbf{V}_1^{\mathrm{inc}} \cdots \mathbf{V}_{N_{\mathrm{rhs}}}^{\mathrm{inc}}]$

More details on the UT Austin EM forward-modeling software:

[3] P. Zhang, J. Shiriyev, Y. Brick, J. Massey, C. Torres-Verdin, A. E. Yılmaz, and M. Sharma, “Fracture diagnostics using a low frequency electromagnetic induction method,” in *Proc. ARMA*, June 2016

[3] A. Menshov, Y. Brick, C. Torres-Verdin, and A. E. Yılmaz, “Recent progress in rigorous algorithms for the fast solution of 3-D EM frequency-domain integral-equations,” to appear in *Proc. 6th Int. Symp. 3-D Electromagnetics*, Mar. 2017.

EM Induction Logging Tool

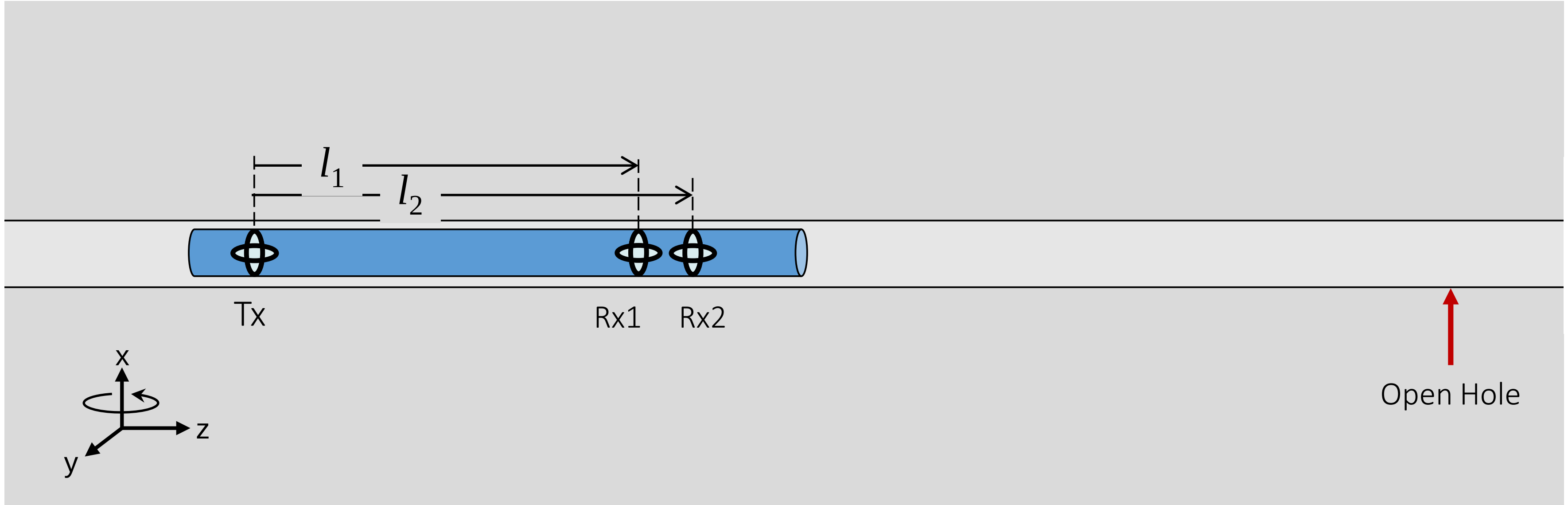

$$\Delta U^{uv} = \mathrm{Re}\left\{-j\omega\mu_o A_{\mathrm{RX}} N_{\mathrm{RX}} \hat{\mathbf{u}} \cdot \left[\mathbf{H}^v\left(\mathbf{r}_{\mathrm{Rx2}}\right) - \mathbf{H}^v\left(\mathbf{r}_{\mathrm{Rx1}}\right)\frac{l_1^3}{l_2^3}\right]\right\}$$

EM Induction Logging Tool

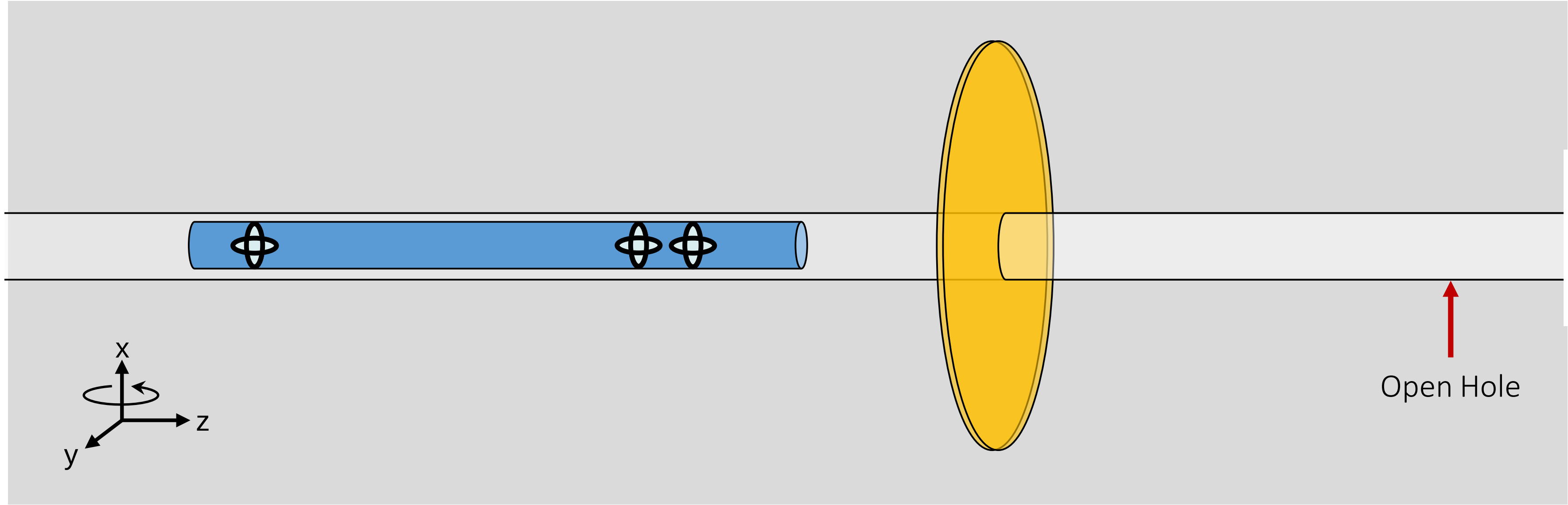

EM Induction Logging Tool

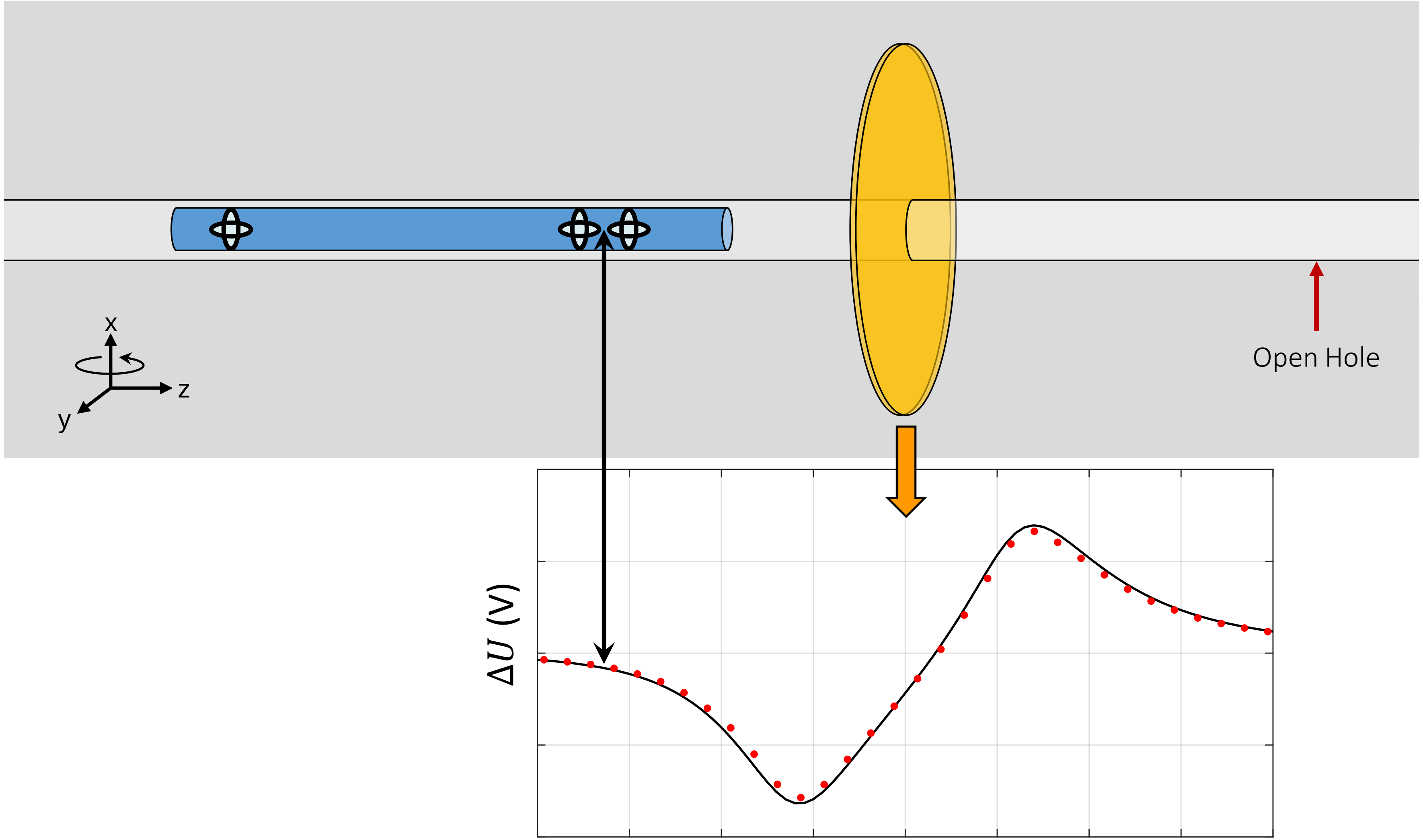

E-Spectrum Technologies

The University of Texas at Austin
Petroleum and Geosystems Engineering

EM Induction Logging Tool

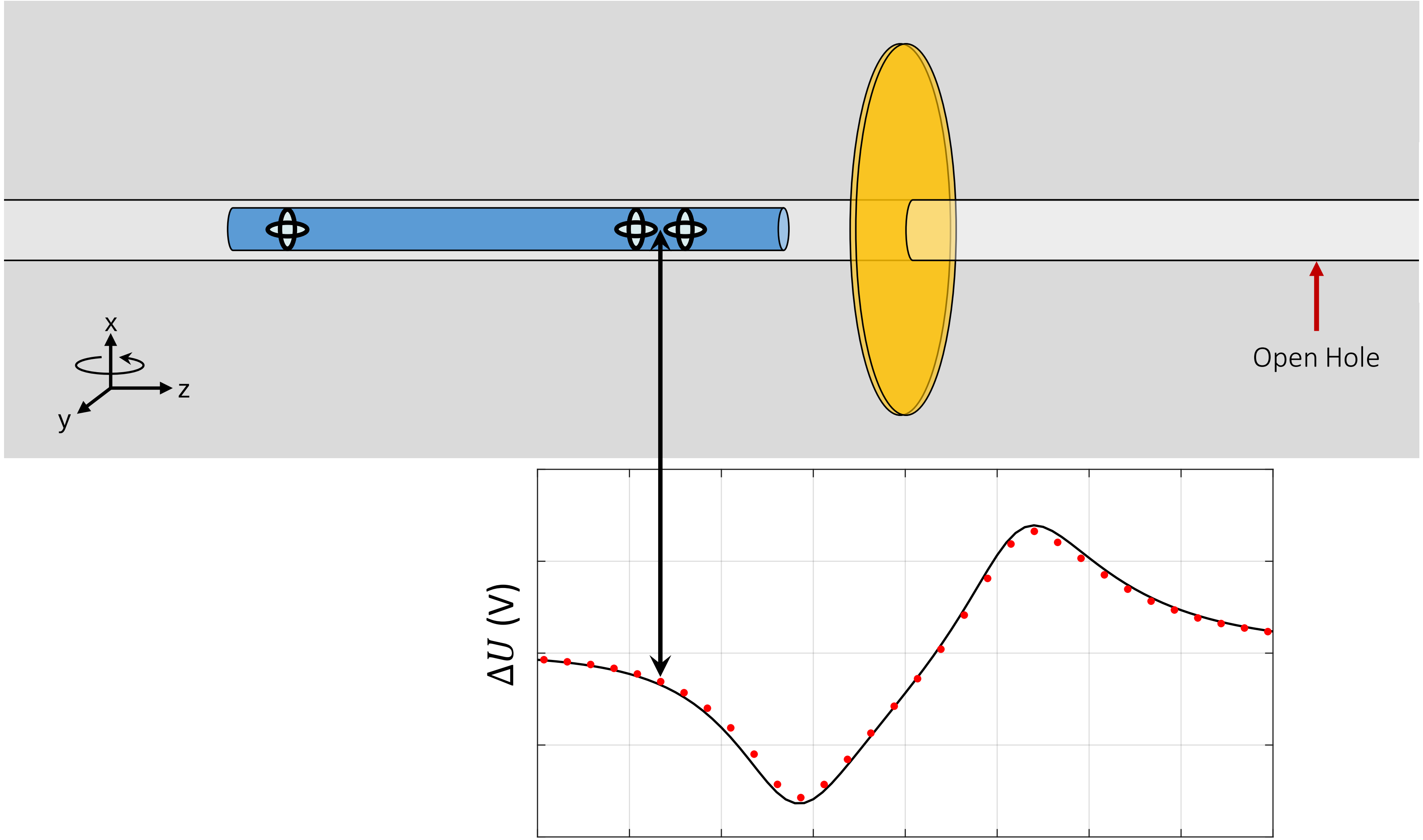

EM Induction Logging Tool

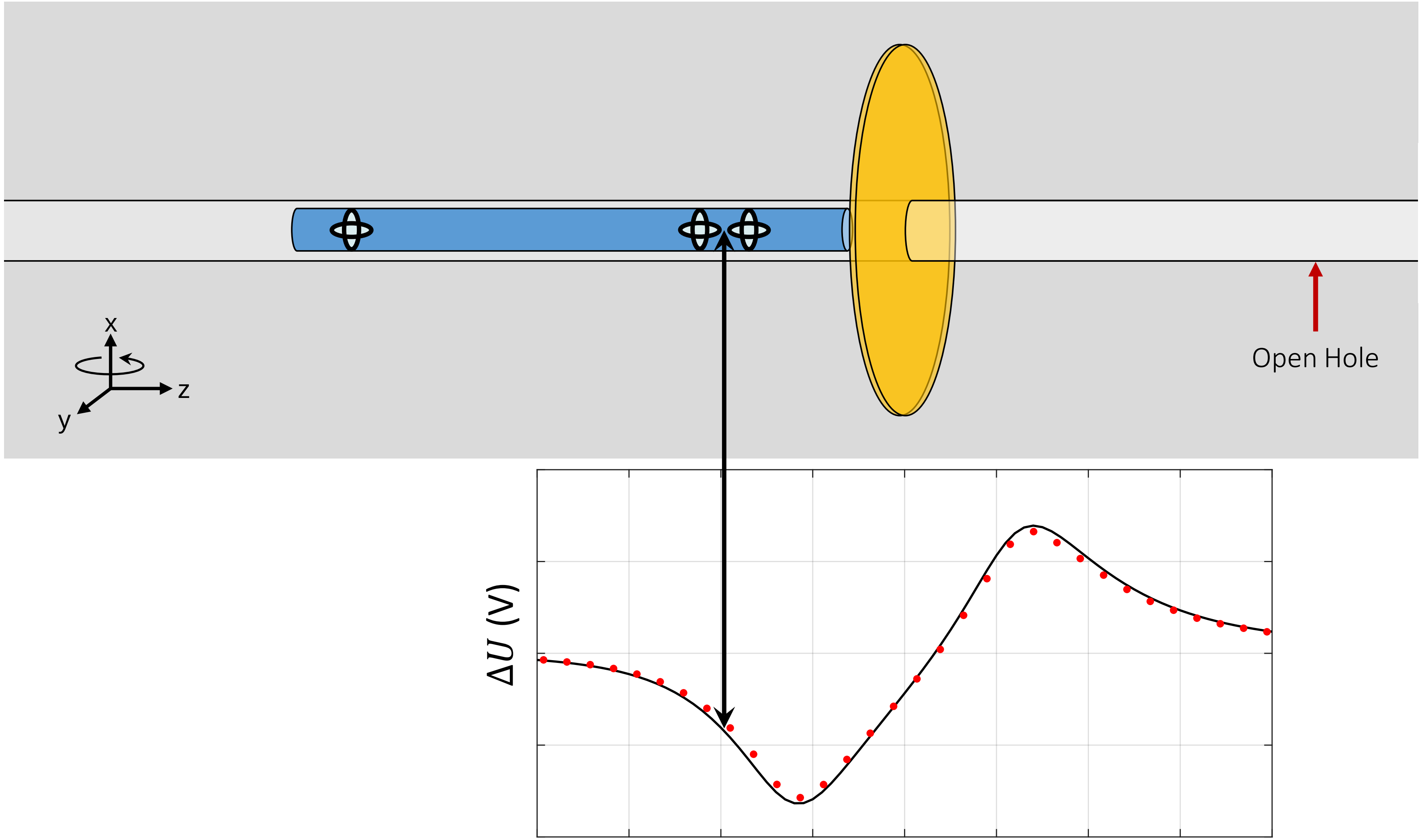

EM Induction Logging Tool

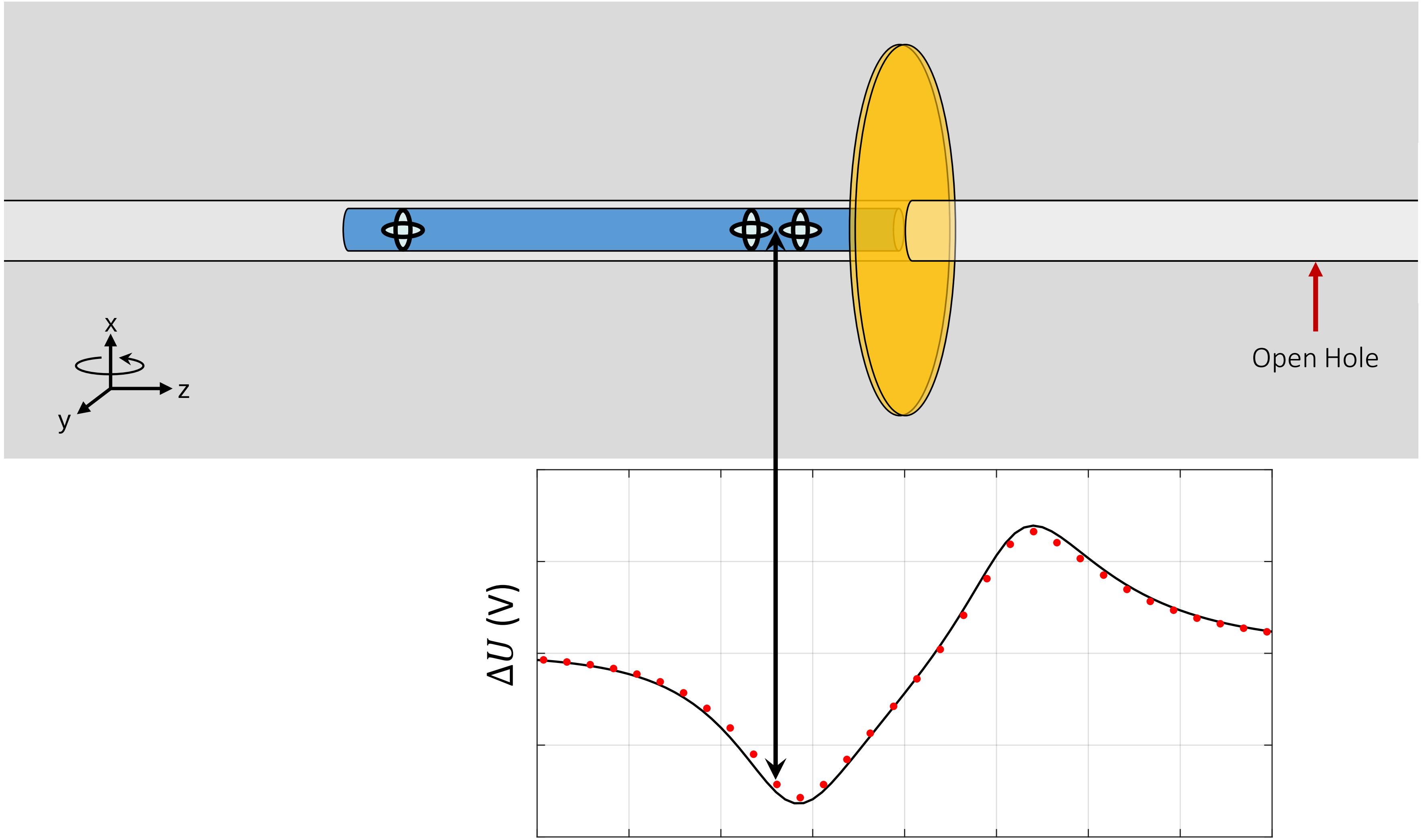

E-Spectrum Technologies

The University of Texas at Austin
Petroleum and Geosystems Engineering

EM Induction Logging Tool

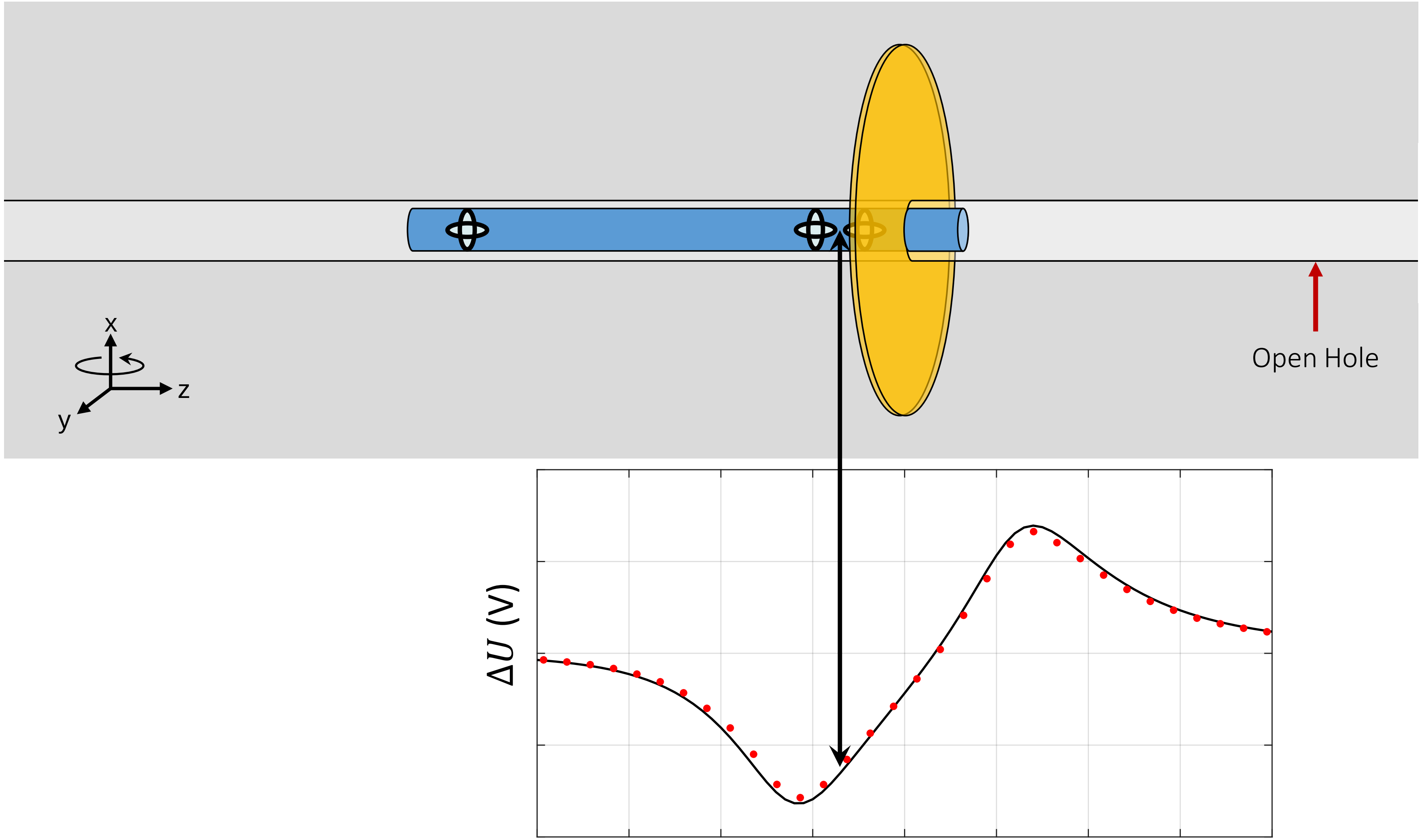

EM Induction Logging Tool

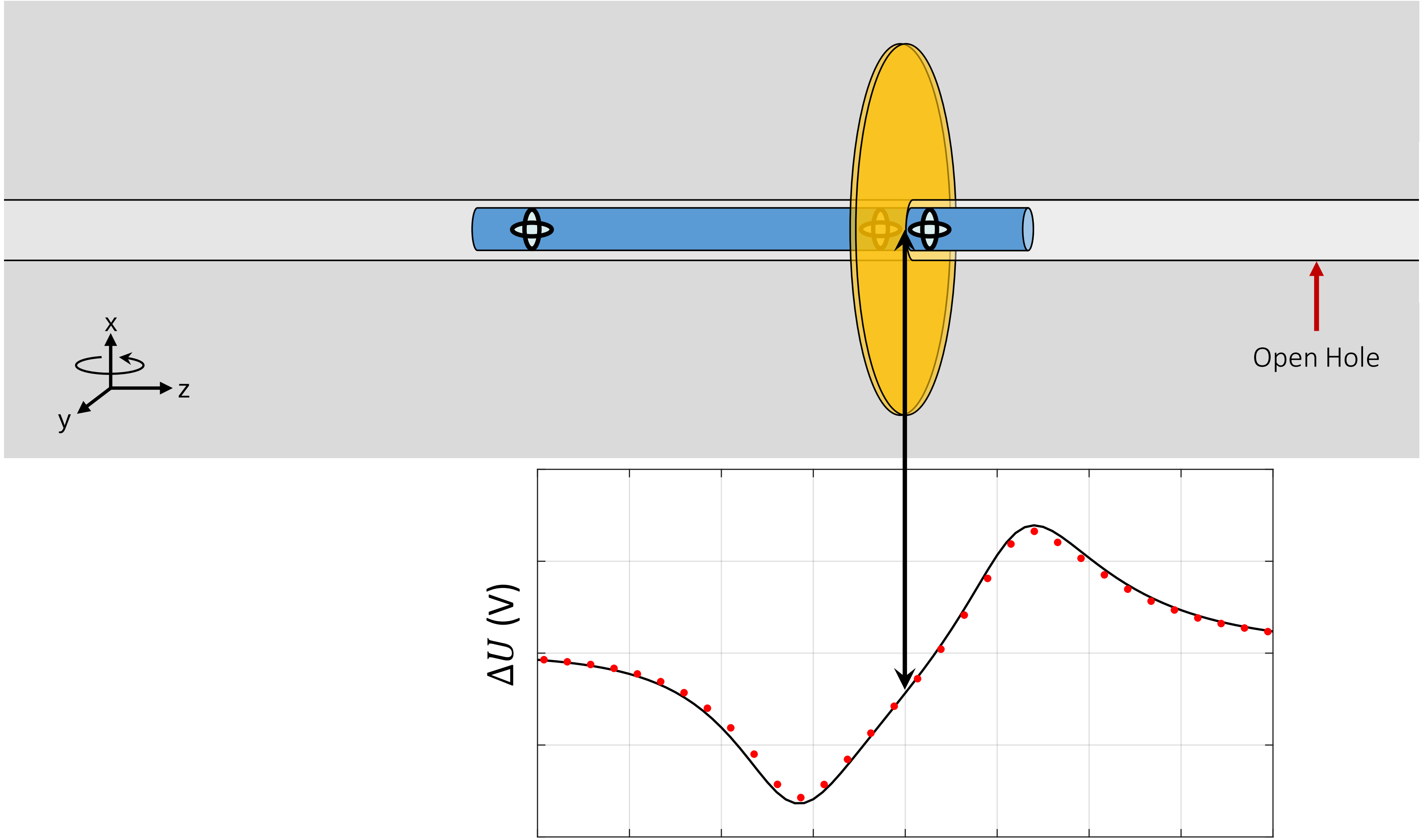

EM Induction Logging Tool

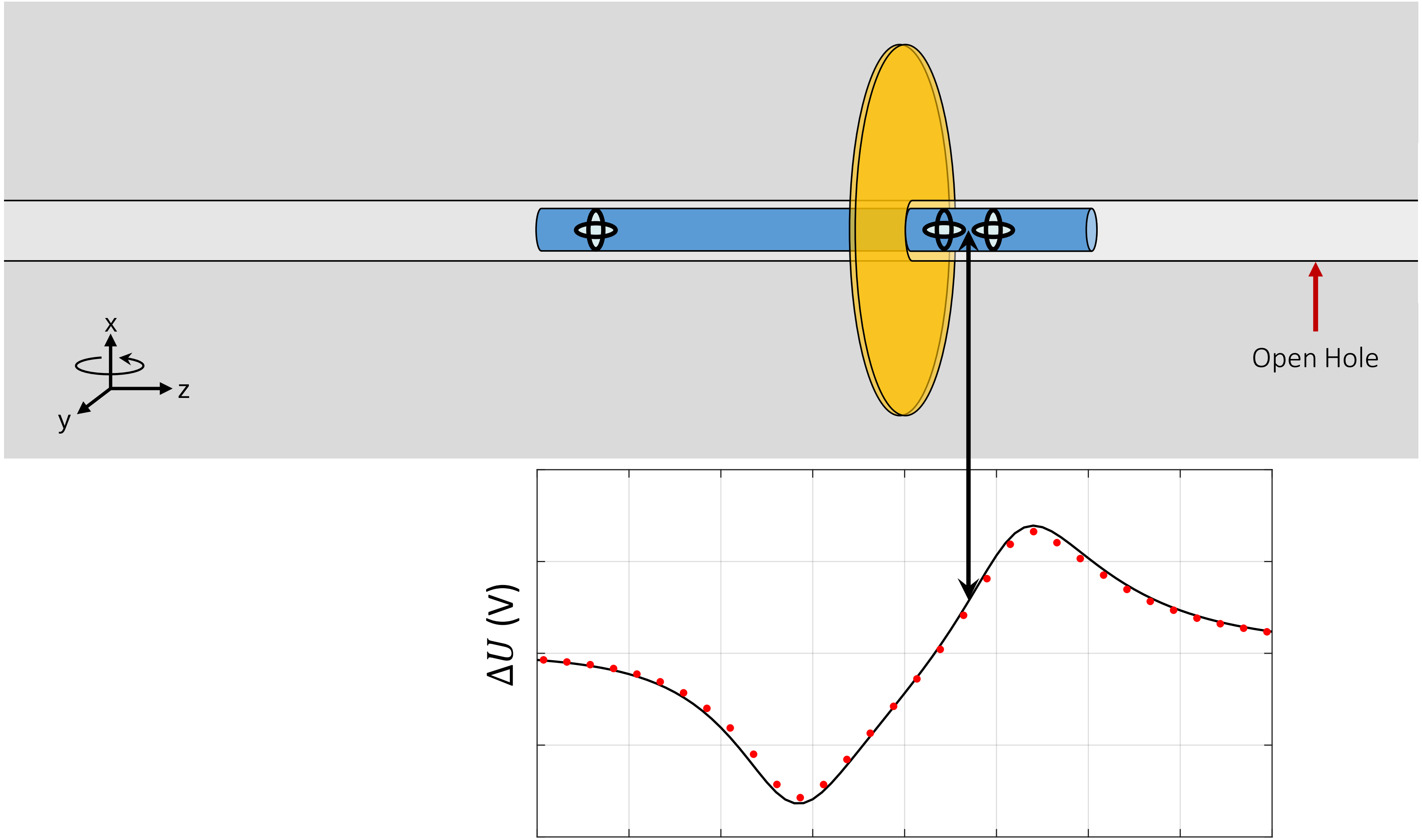

E-Spectrum Technologies

The University of Texas at Austin
Petroleum and Geosystems Engineering

EM Induction Logging Tool

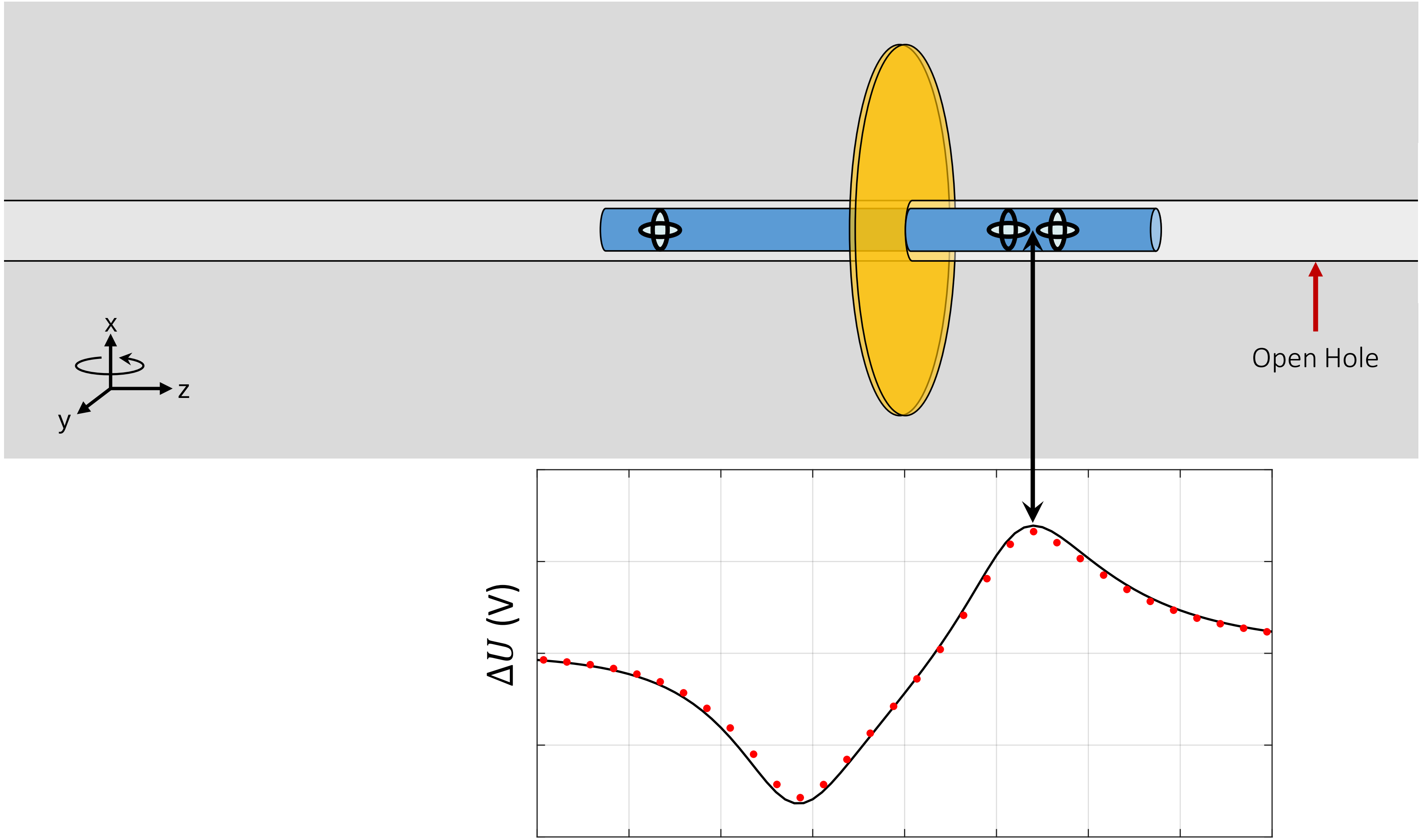

EM Induction Logging Tool

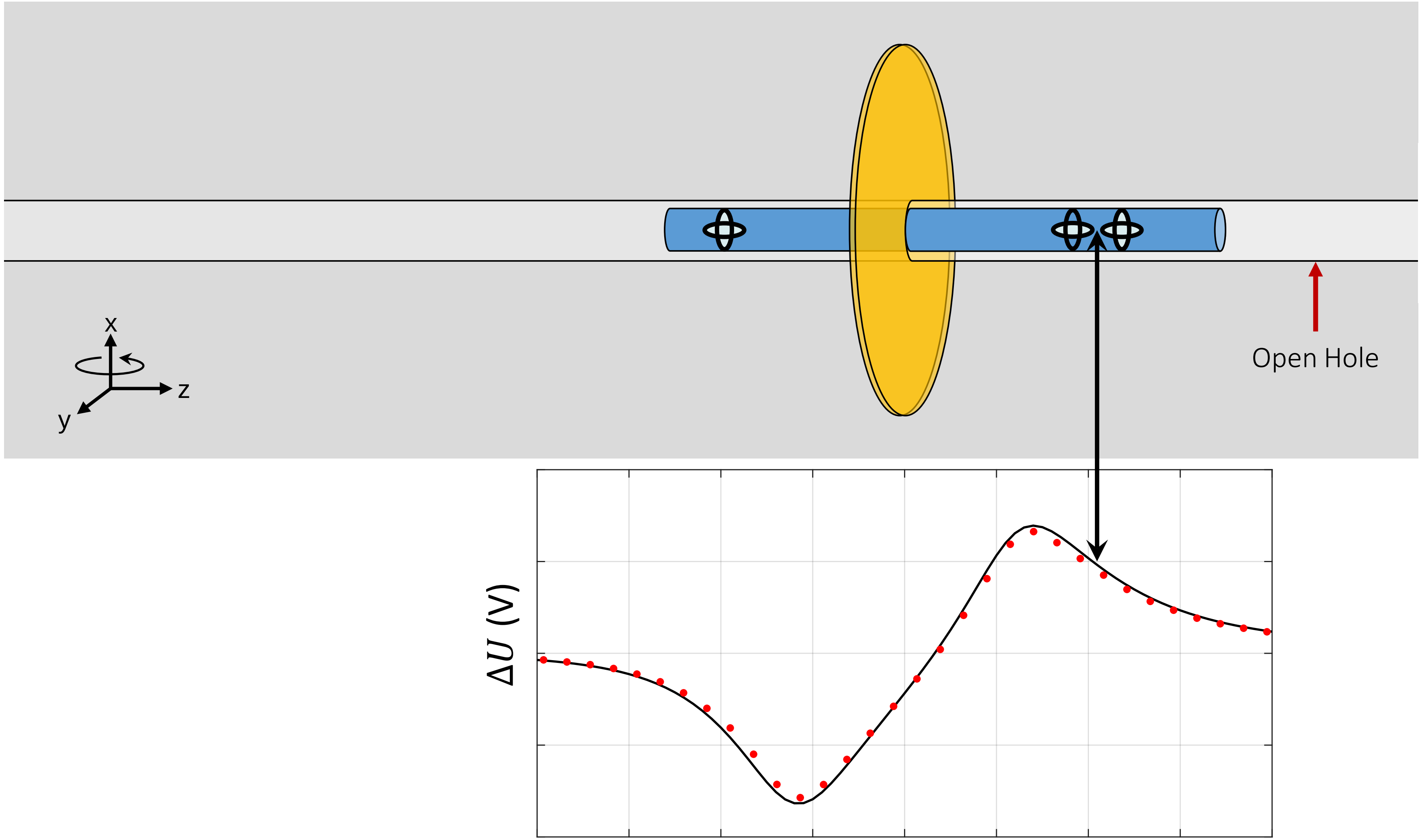

E-Spectrum Technologies

The University of Texas at Austin
Petroleum and Geosystems Engineering

EM Induction Logging Tool

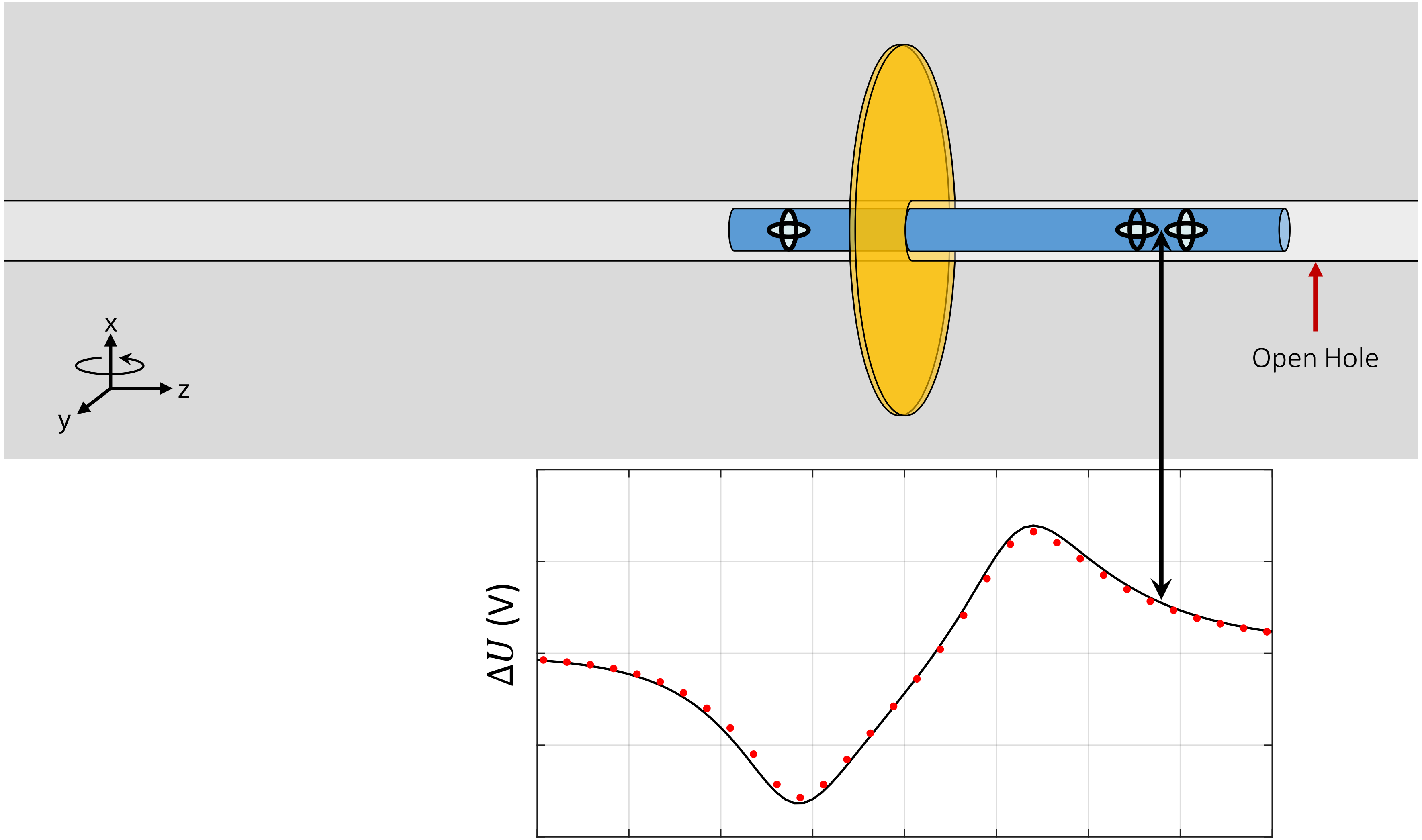

EM Induction Logging Tool

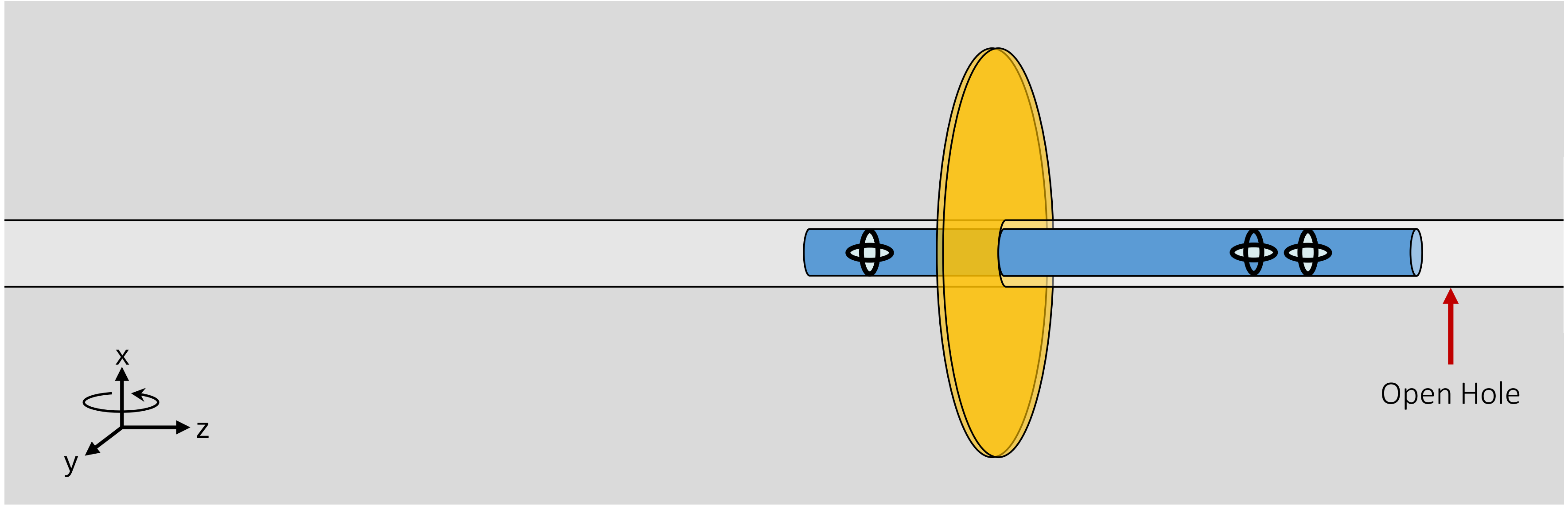

$$\Delta U^{uv} = \mathrm{Re}\left\{-j\omega\mu_o A_{\mathrm{RX}} N_{\mathrm{RX}} \hat{\mathbf{u}} \cdot \left[\mathbf{H}^{v}\left(\mathbf{r}_{\mathrm{Rx2}}\right) - \mathbf{H}^{v}\left(\mathbf{r}_{\mathrm{Rx1}}\right) \frac{l_1^3}{l_2^3}\right]\right\}$$

$$\Delta U_{\mathrm{diff}}^{uv} = \left|\Delta U_{\mathrm{frac}}^{uv} - \Delta U_{\mathrm{bore}}^{uv}\right| \geq V_{\mathrm{resolution}}$$

$$\alpha^{uv} = \Delta U_{\mathrm{diff}}^{uv} / \Delta U_{\mathrm{bore}}^{zz} \geq n = 2\,\%$$

EM Induction Logging Tool

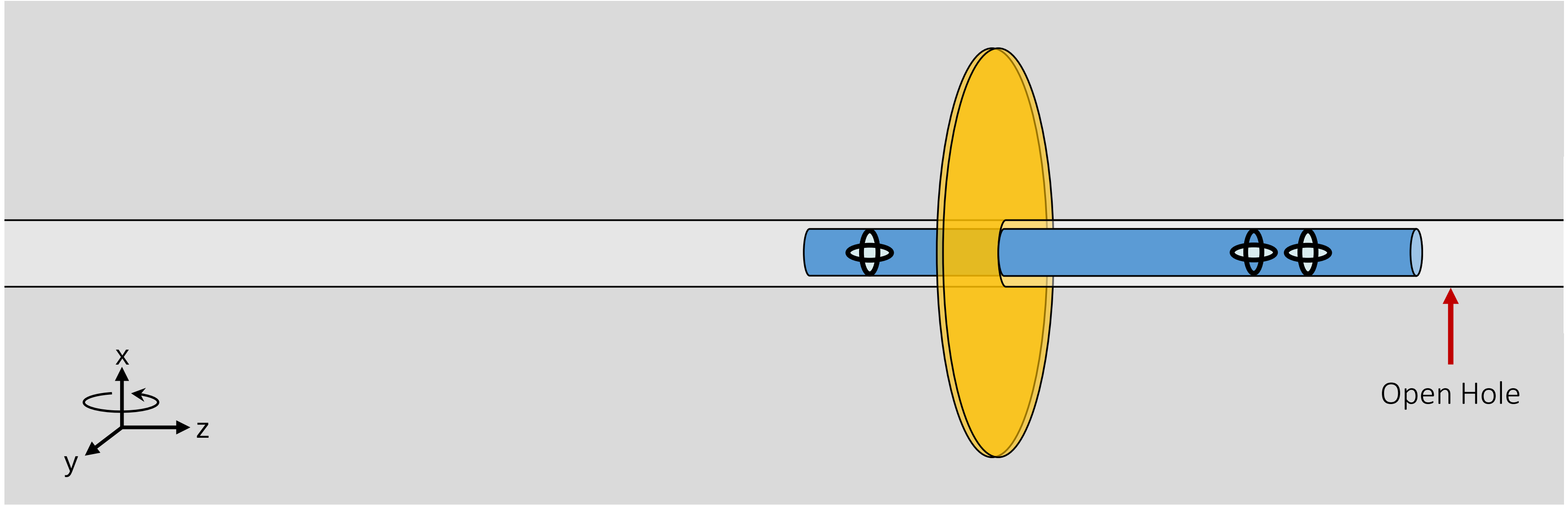

$$\Delta U^{uv} = \mathrm{Re}\left\{-j\omega\mu_o A_{\mathrm{RX}} N_{\mathrm{RX}} \hat{\mathbf{u}} \cdot \left[\mathbf{H}^{v}\left(\mathbf{r}_{\mathrm{Rx2}}\right) - \mathbf{H}^{v}\left(\mathbf{r}_{\mathrm{Rx1}}\right)\frac{l_1^3}{l_2^3}\right]\right\}$$

$$\Delta U_{\mathrm{diff}}^{uv} = \left|\Delta U_{\mathrm{frac}}^{uv} - \Delta U_{\mathrm{bore}}^{uv}\right| \geq V_{\mathrm{resolution}}$$

$$\alpha^{uv} = \Delta U_{\mathrm{diff}}^{uv} / \Delta U_{\mathrm{bore}}^{zz} \geq n = 2\ \%$$

Short Spacing
$l_1 = 1.2$ m $l_2 = 1.5$ m

Intermediate Spacing
$l_1 = 5.0$ m $l_2 = 5.6$ m

Long Spacing
$l_1 = 18.0$ m $l_2 = 19.2$ m

Tasks

- Task 1.0 -- Project Management Plan
- Task 2.0 - Development of forward model using proposed tool and different fracture geometries
- Task 3.0 - Lab testing of available proppants in the market for electrical and material properties
- Task 4.0 – Final design and construction of low frequency electromagnetic tool
- Task 5.0 – Laboratory and field testing of tool
- Task 6.0 -- Inverting the field data to obtain the fracture geometry

E-Spectrum Technologies

The University of Texas at Austin
Petroleum and Geosystems Engineering

Tool Construction and Lab Testing

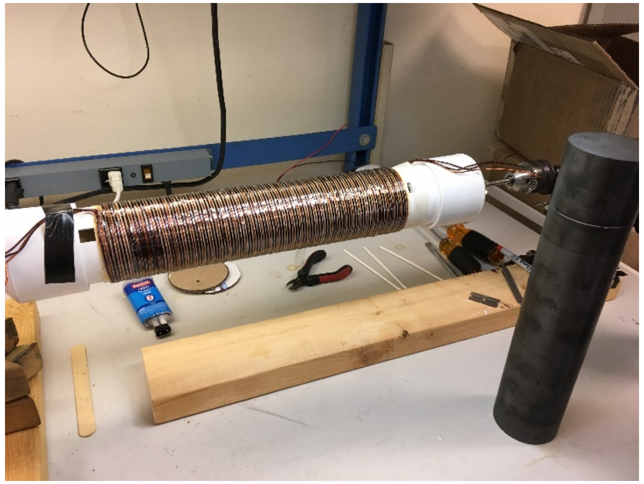

Axial TX coil on winding fixture with ferrite core to the side

Tank circuit, transmit coil with capacitor board on the right

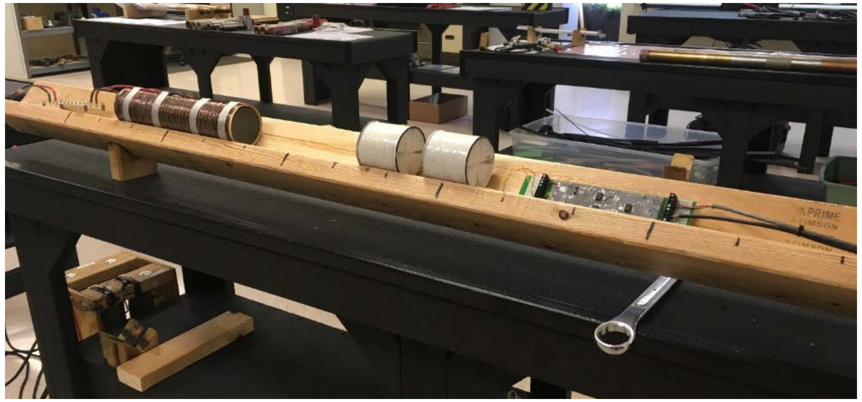

Initial bench testing of TX-RX coil setup

Co-planar coil after construction

RX coils:
z-coil (right)
x/y coil (left)

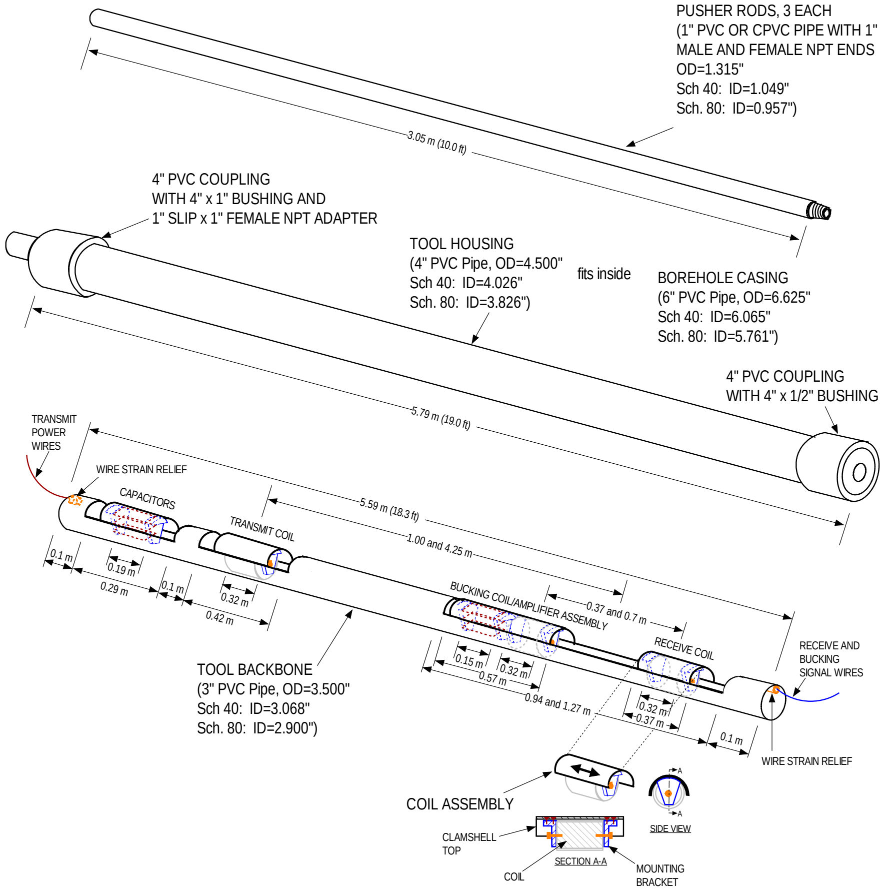

Lab test fixture diagram for LFIE tool

Comparison of Lab Results with Simulations

E-Spectrum Technologies

The University of Texas at Austin
Petroleum and Geosystems Engineering

Comparison of Lab Results with Simulations

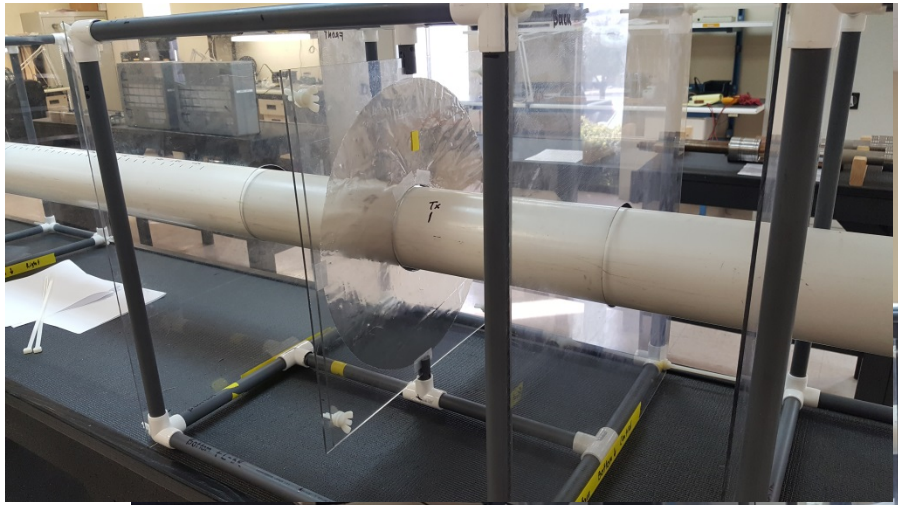

– **Industrial Aluminum Foil**
Conductivity at 20°C: 33.4 – 35.8 MS/m
Thickness: 25.4 ± 10% μm
– **Fracture Holder:** Plexiglass acrylic sheet

Lab test fixture for LFEI tool

Comparison of Lab Results with Simulations

Power Amplifier

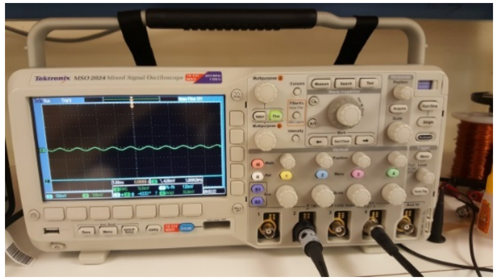

Tektronix
MSO-scope 2024

Pre-amp PCB

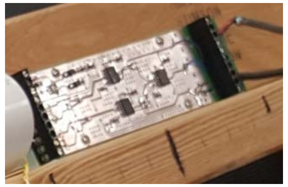

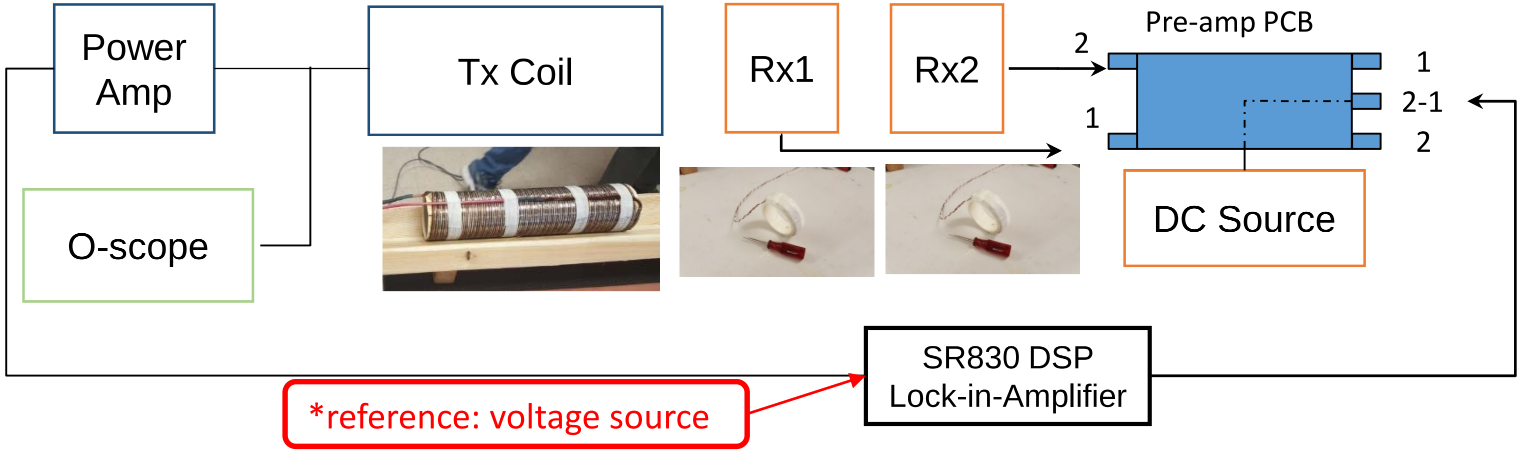

SR830 DSP
Lock-in-Amplifier

Lab Measurements

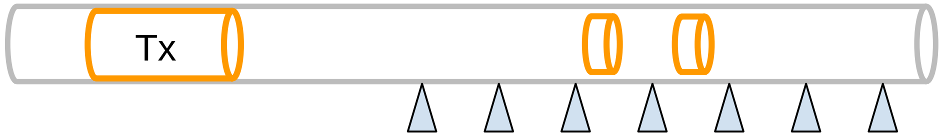

- All coils have been tested to verify the given properties.
- A single coil configuration is tested at a time
- Transmitter coil currents are measured during tests and results are normalized with respect to currents.
- At every sampling point data have been recorded for a minute at least and signal to noise ratio is shown to be strong.
- Signals are referenced with respect to voltage around the transmitter coil. Reference phase is used to rotate the output channels to get in-phase (real) and quadrature (imaginary) components of received signals.

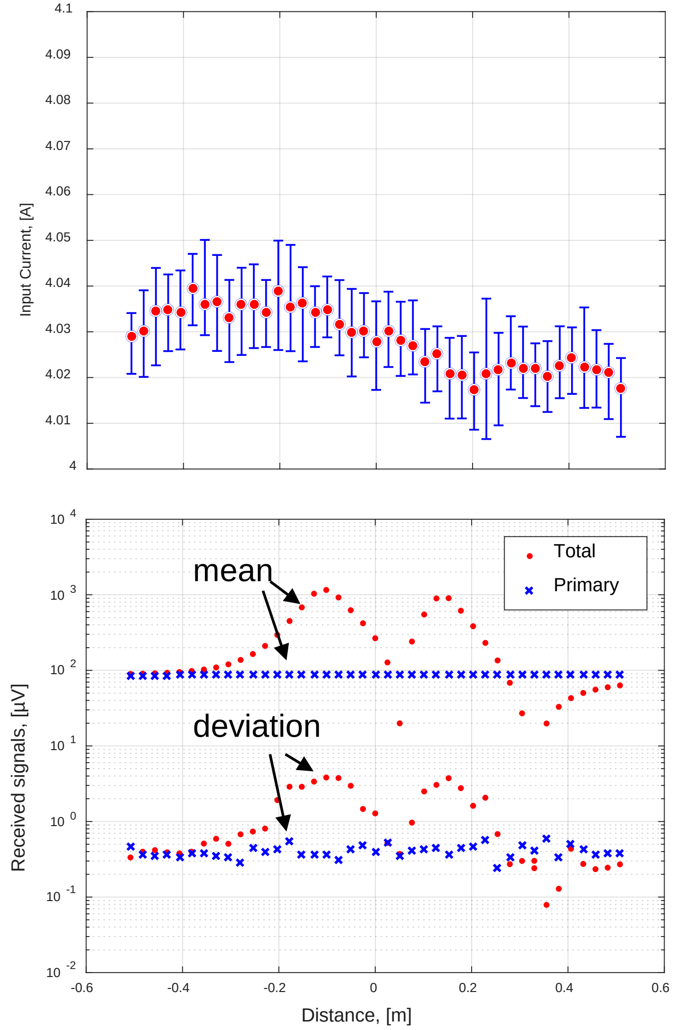

Fracture Lab / Subsurface Models

– **Industrial Aluminum Foil**
Conductivity at 20°C is $33.4 - 35.8\ \mathrm{MS/m}$
Thickness is $25.4 \pm 10\%\ \mu\mathrm{m}$
(also verified with micrometer measurement)

– **Experiment setup**
Plexiglass, PVC pipes, nylon rod and Lexan

– **Comparison to real size hydraulic fractures**

a) Circular Fractures

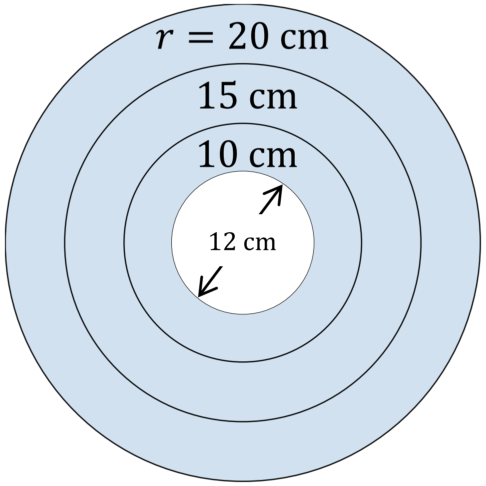

b) Elliptical Fractures

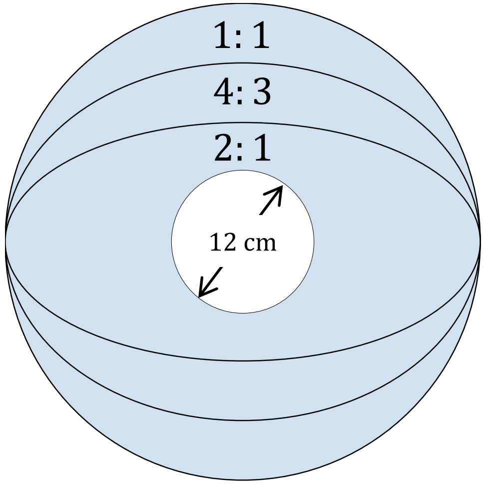

c) Rotated Fractures

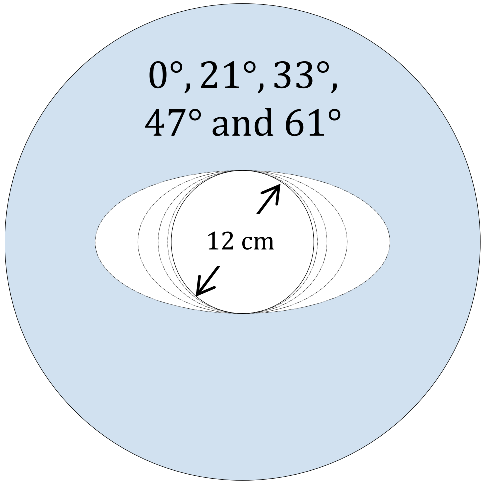

d) Subsurface Model

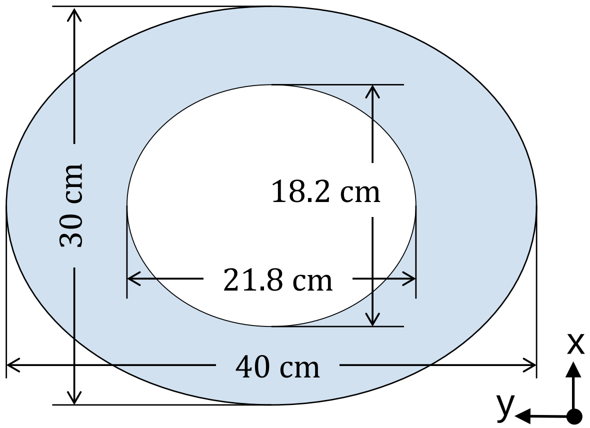

Comparison of Lab Results with Simulations

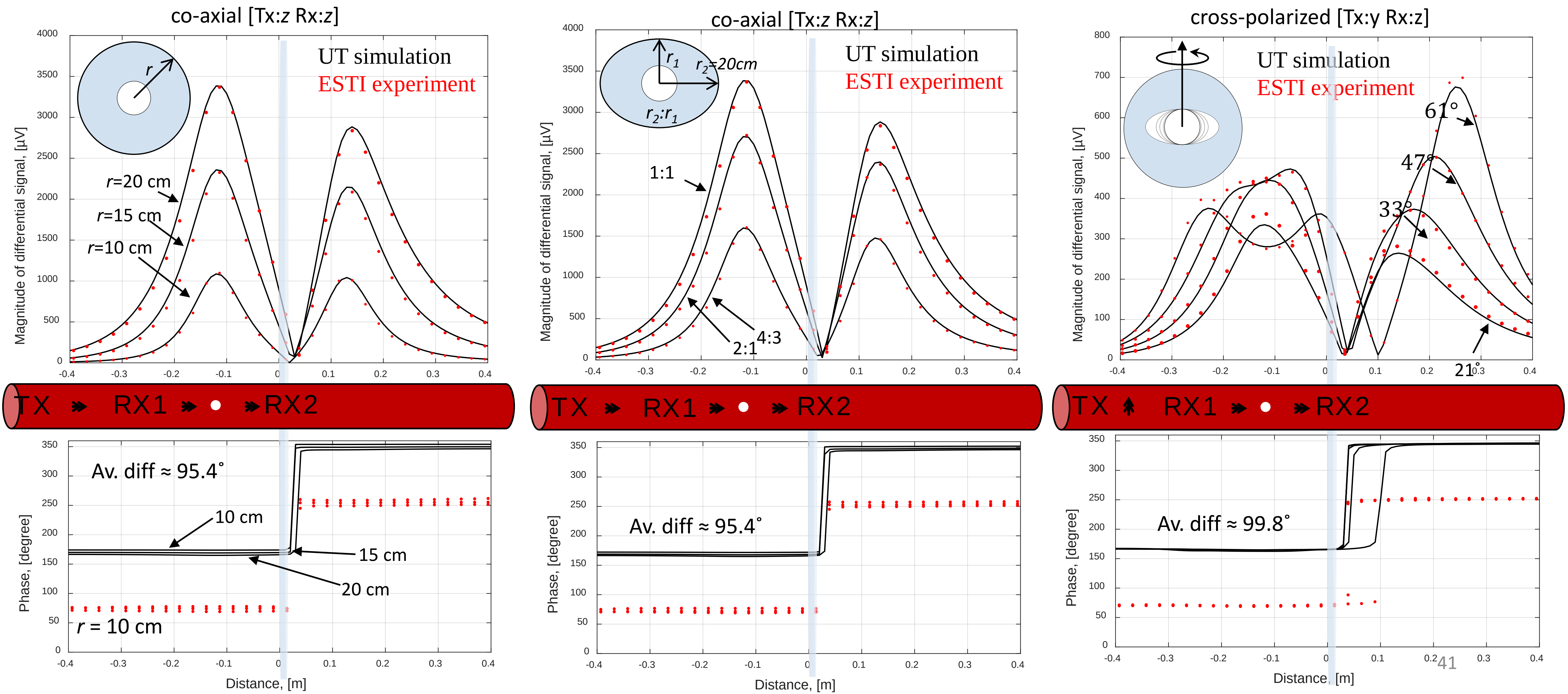

Results – Lab Measurements

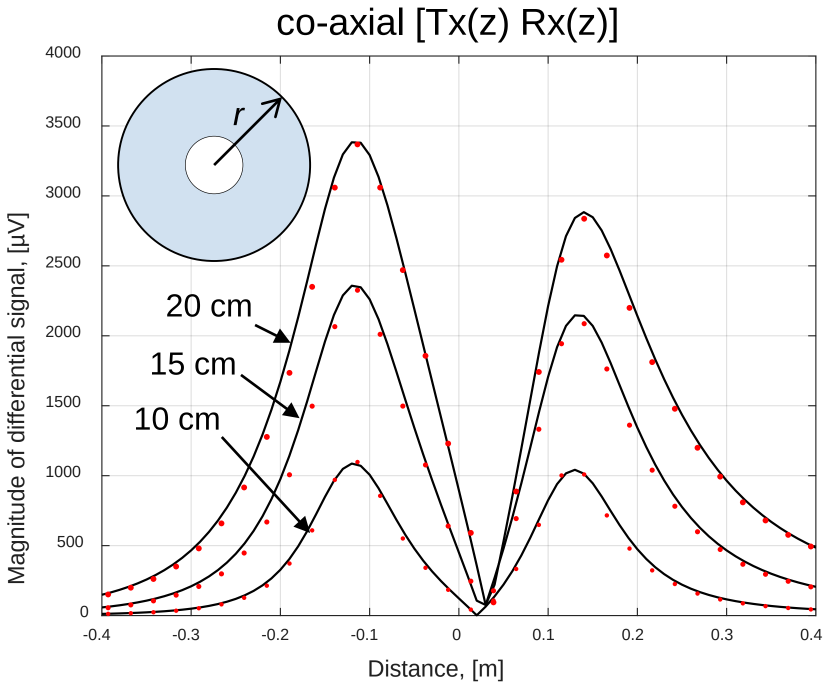

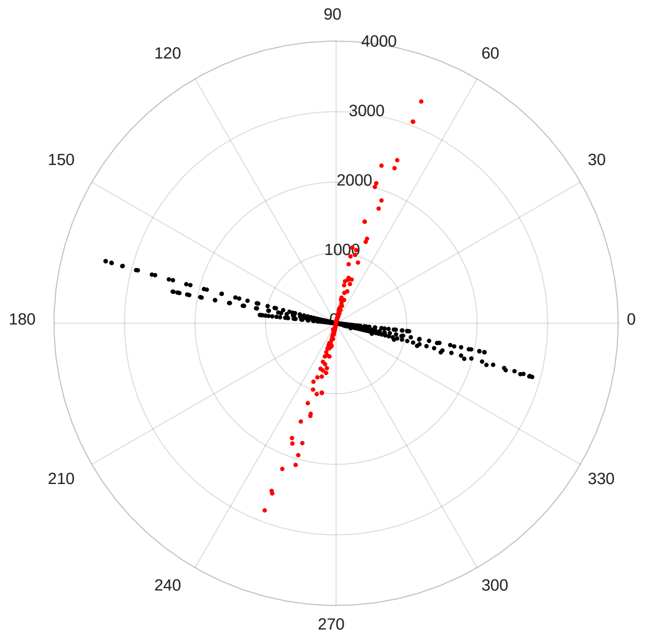

Parameter	Co-Axial	Co-Planar	Cross-Polarized
Surface Area	>100 µV	>10 µV	<1 µV
Aspect Ratio	>100 µV	>10 µV	<1 µV
Dip Angle	>100 µV	>100 µV	>100 µV

Results – Lab Measurements

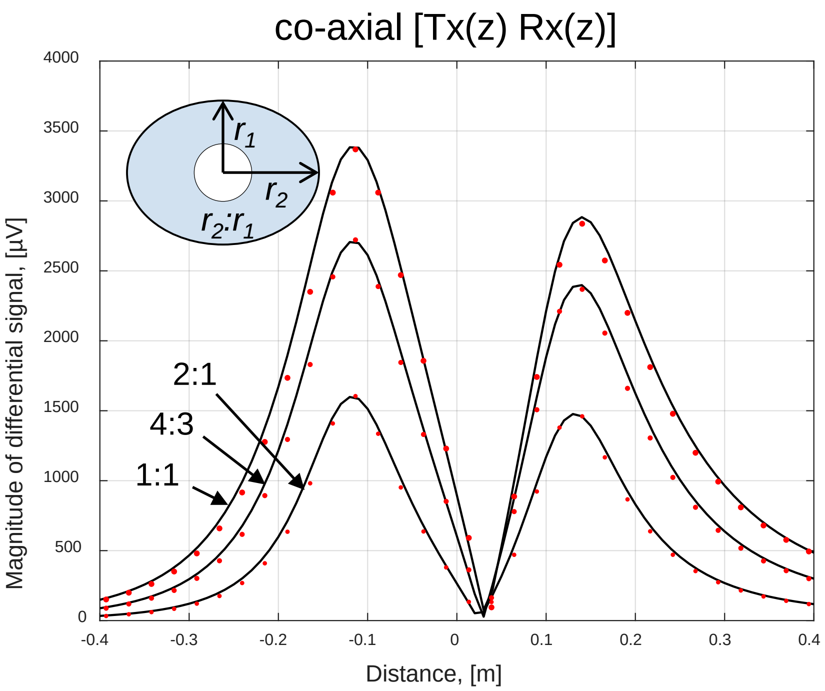

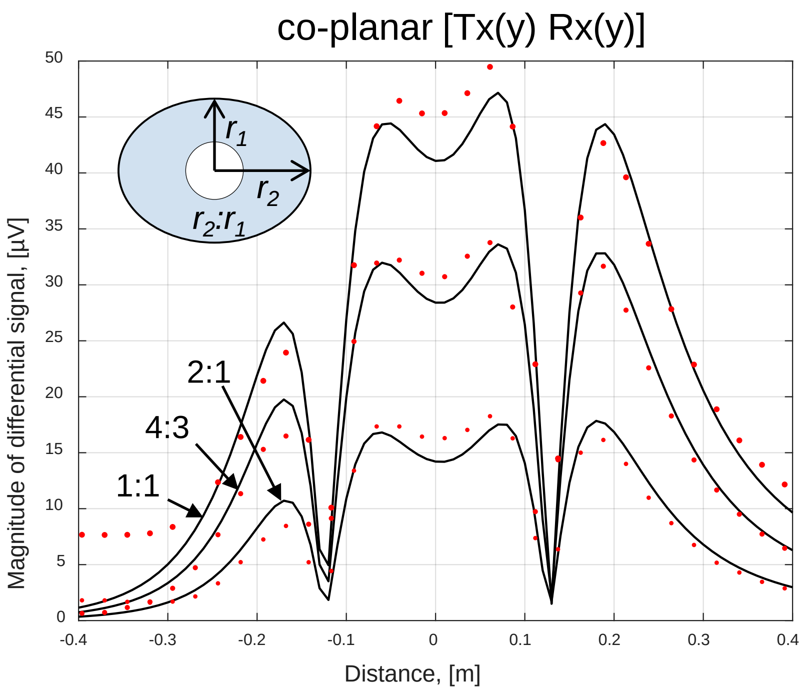

Parameter	Co-Axial	Co-Planar	Cross-Polarized
Surface Area	>100 μV	>10 μV	<1 μV
Aspect Ratio	>100 μV	>10 μV	<1 μV
Dip Angle	>100 μV	>100 μV	>100 μV

Results – Lab Measurements

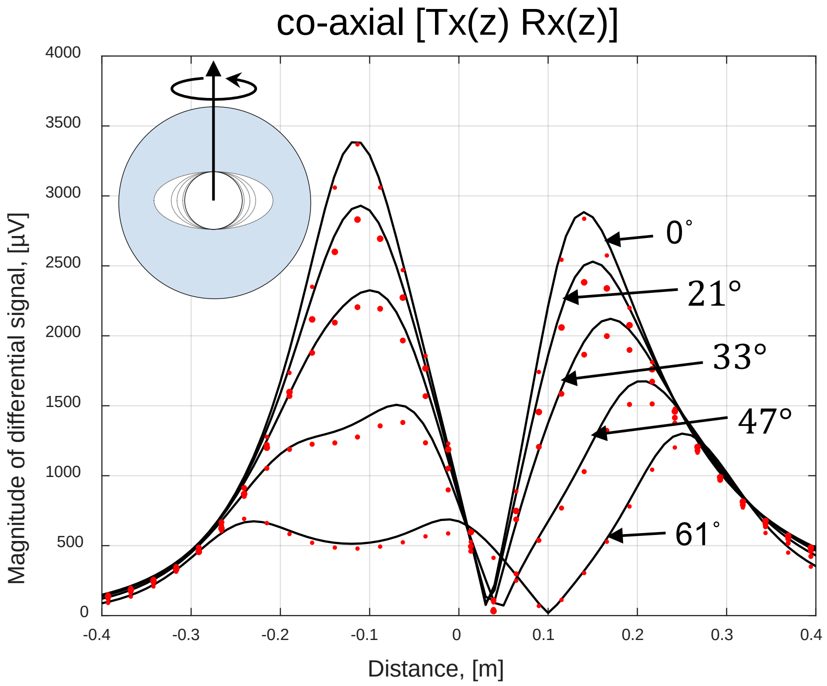

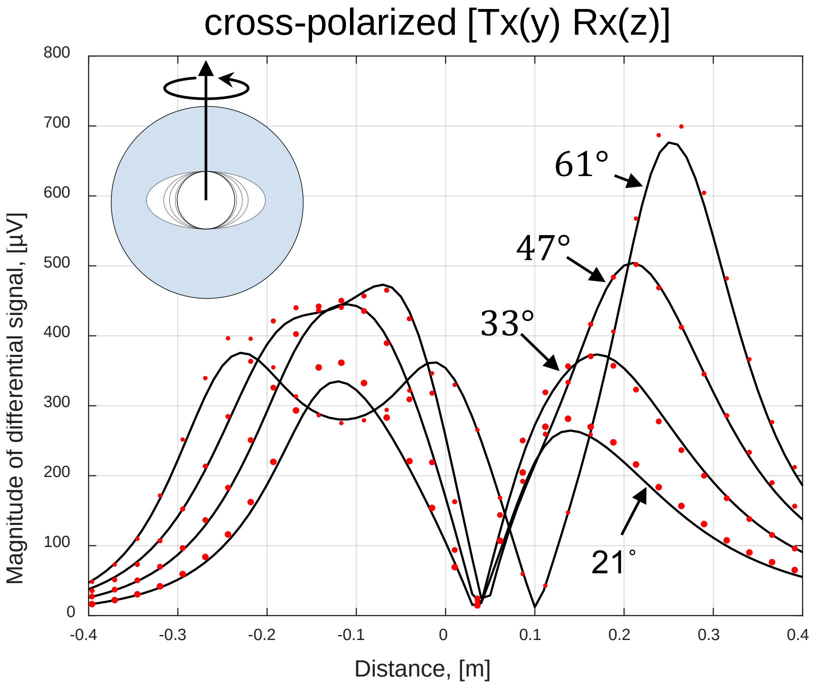

Parameter	Co-Axial	Co-Planar	Cross-Polarized
Surface Area	>100 µV	>10 µV	<1 µV
Aspect Ratio	>100 µV	>10 µV	<1 µV
Dip Angle	>100 µV	>100 µV	>100 µV

Tasks

- Task 1.0 -- Project Management Plan
- Task 2.0 - Development of forward model using proposed tool and different fracture geometries
- Task 3.0 - Lab testing of available proppants in the market for electrical and material properties
- Task 4.0 – Final design and construction of low frequency electromagnetic tool
- Task 5.0 – Laboratory and field testing of tool
- Task 6.0 -- Inverting the field data to obtain the fracture geometry

Near-surface field testing (Task 5)

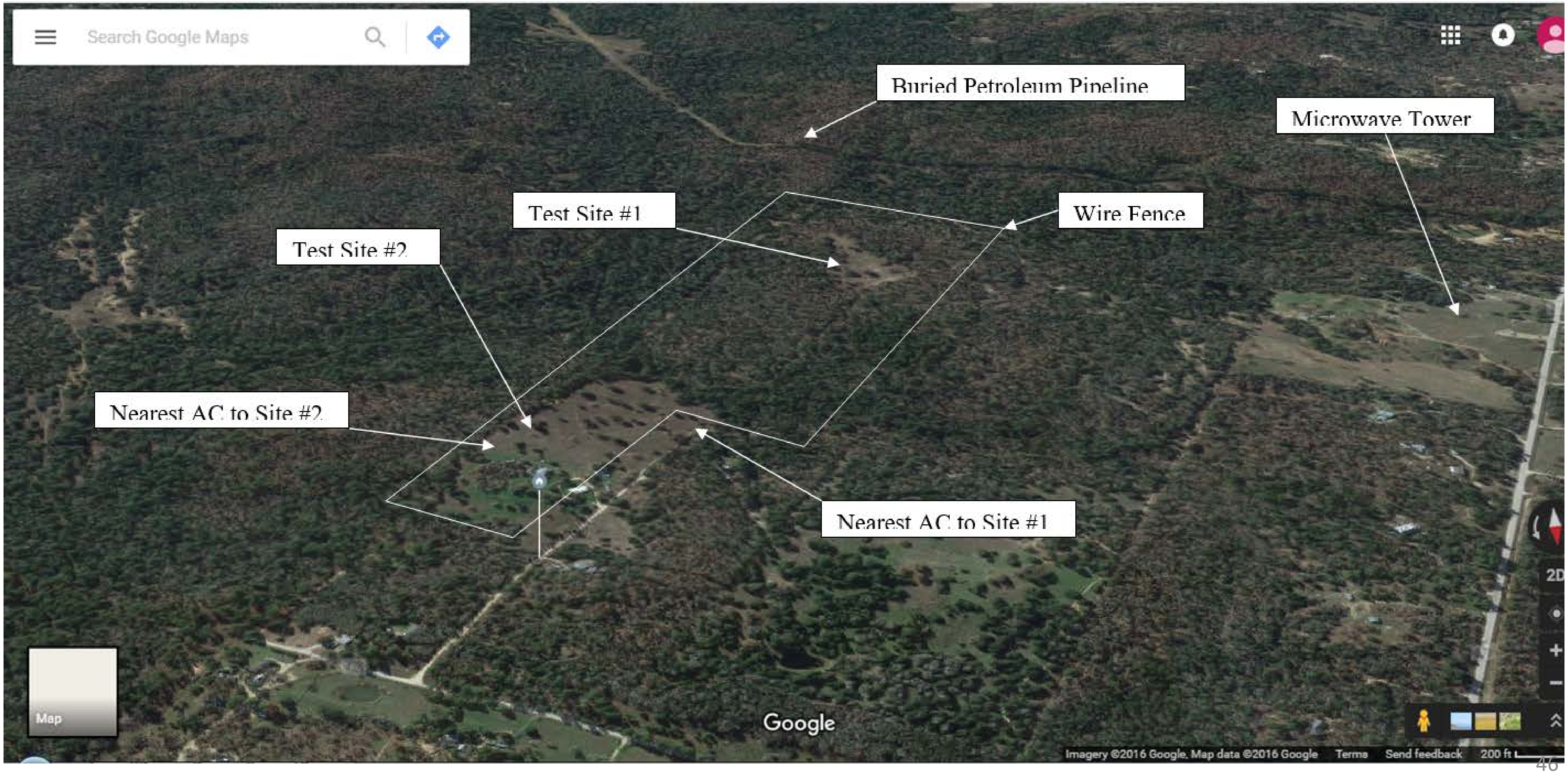

Subsurface Measurements

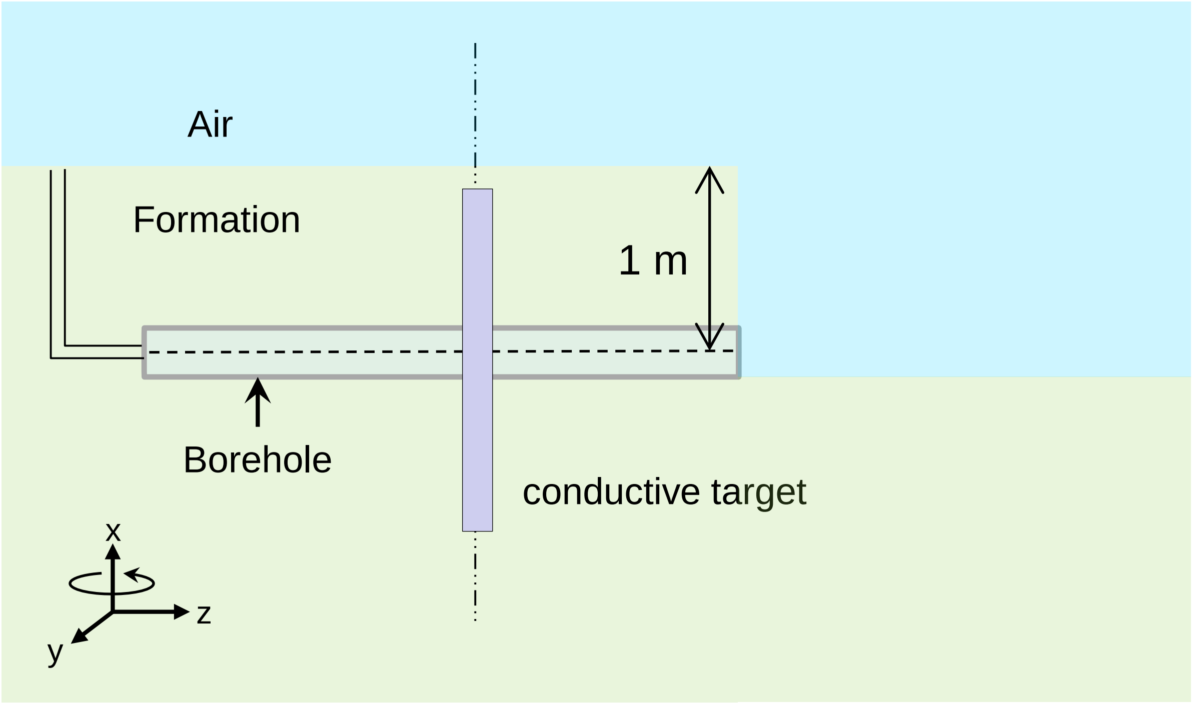

Subsurface Measurements

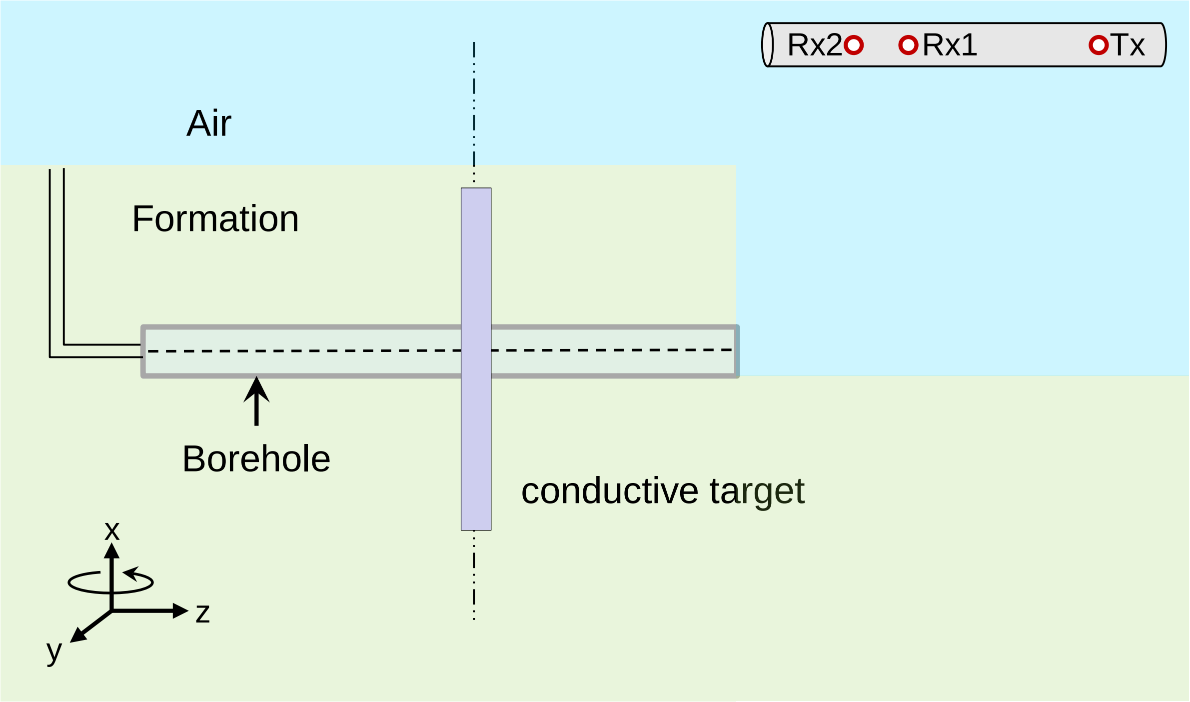

Subsurface Measurements

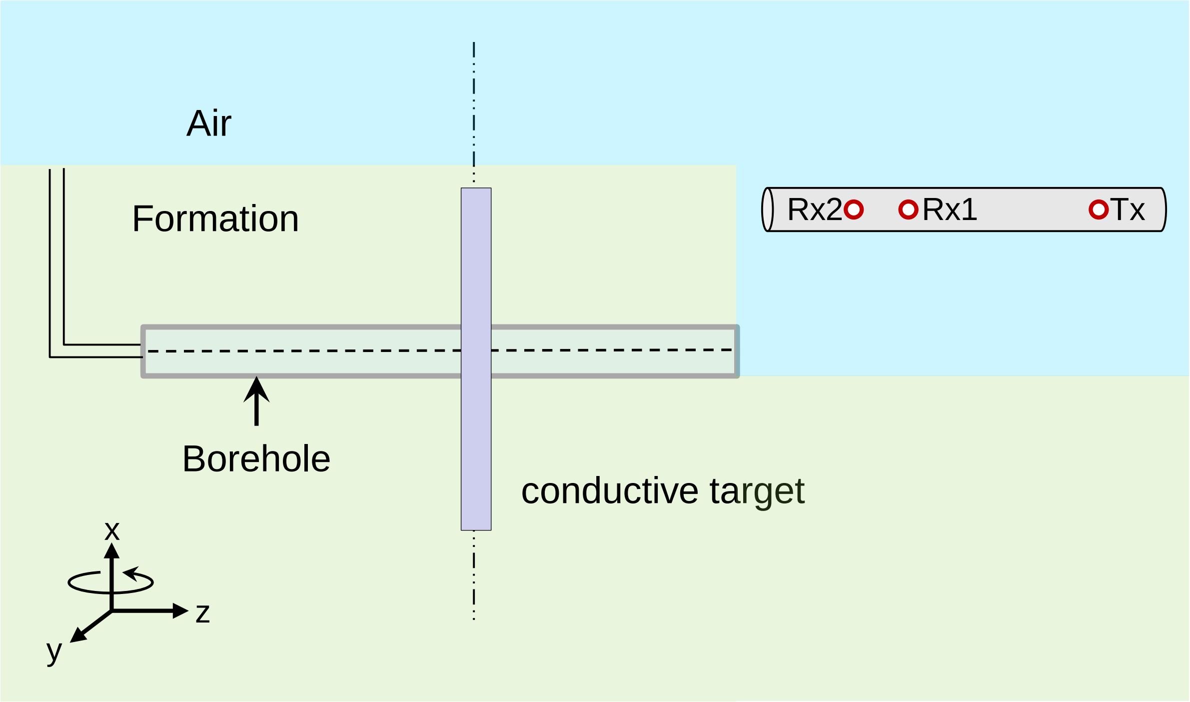

Subsurface Measurements

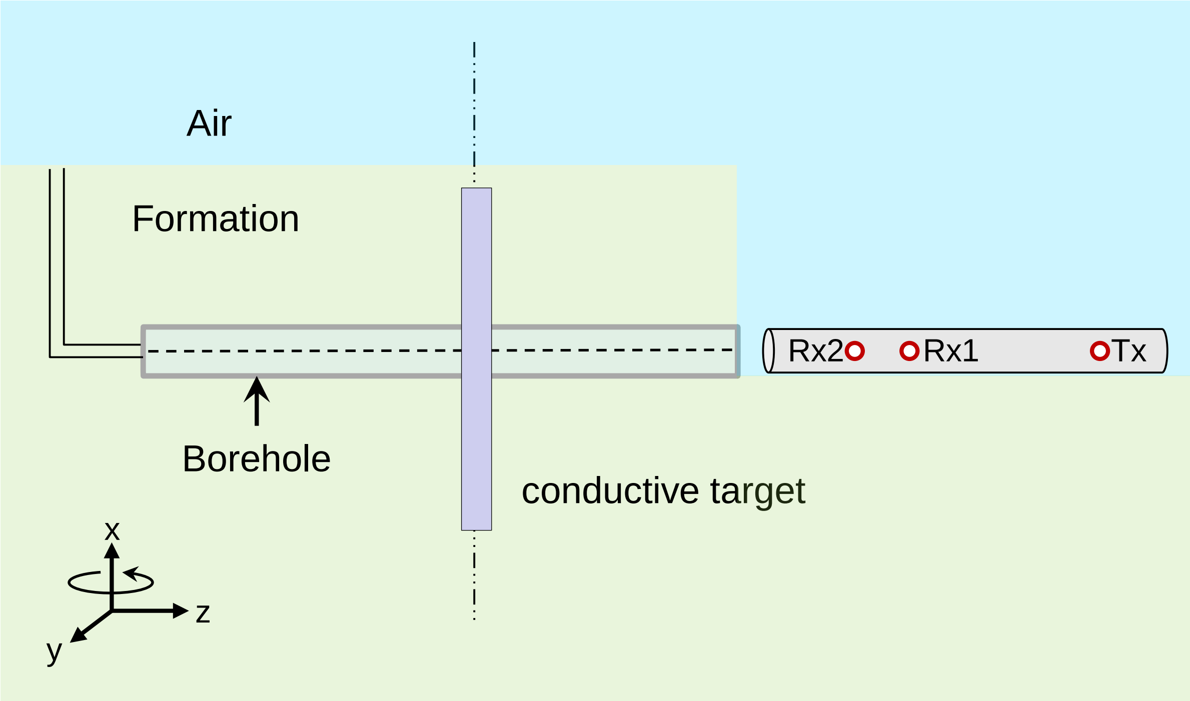

Subsurface Measurements

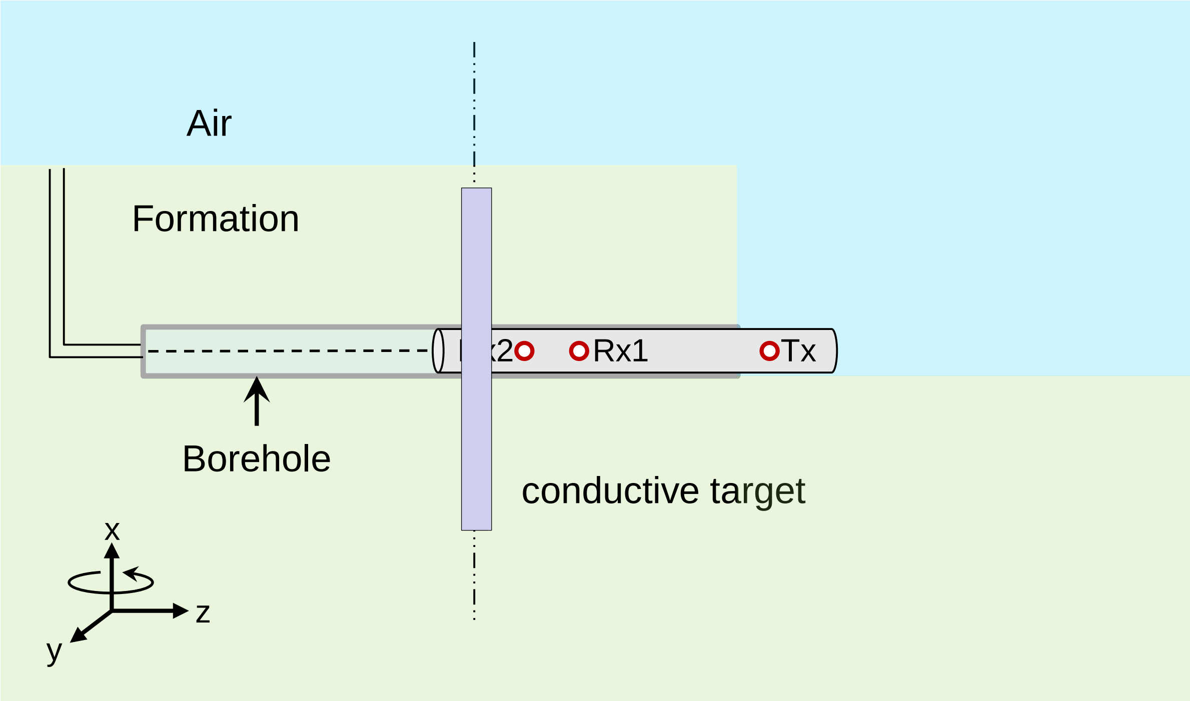

Subsurface Measurements

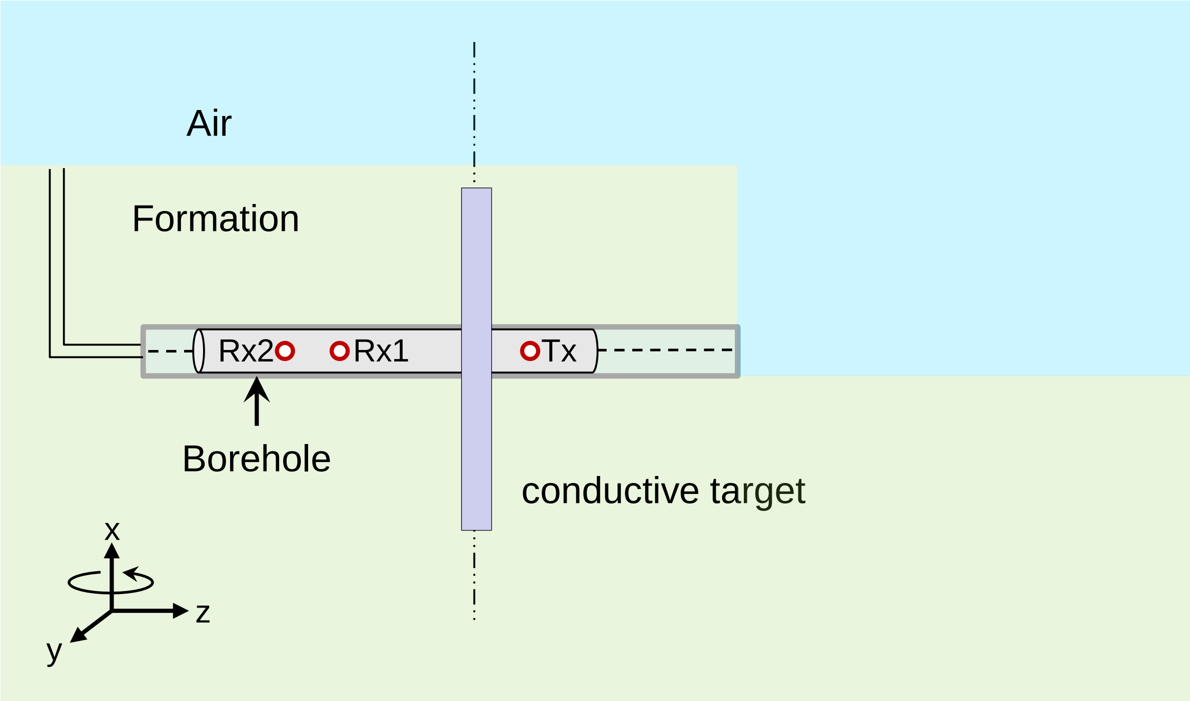

Near-surface field testing (Task 5)

Uncovering the partially collapsed slot box and installing the 2X10 support beams.

Results – Subsurface Measurements

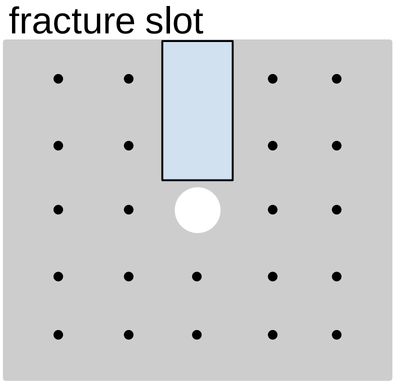

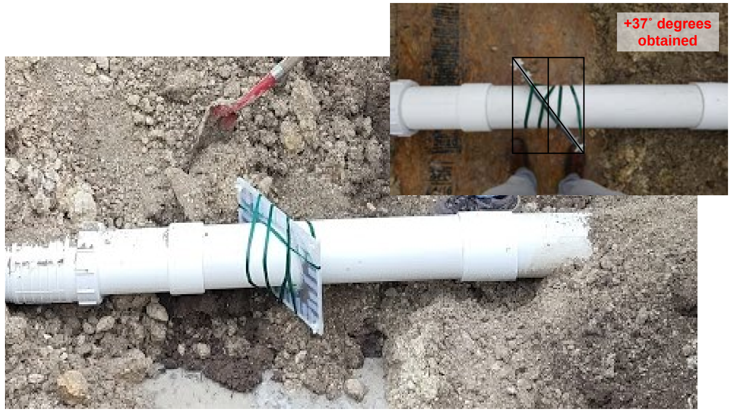

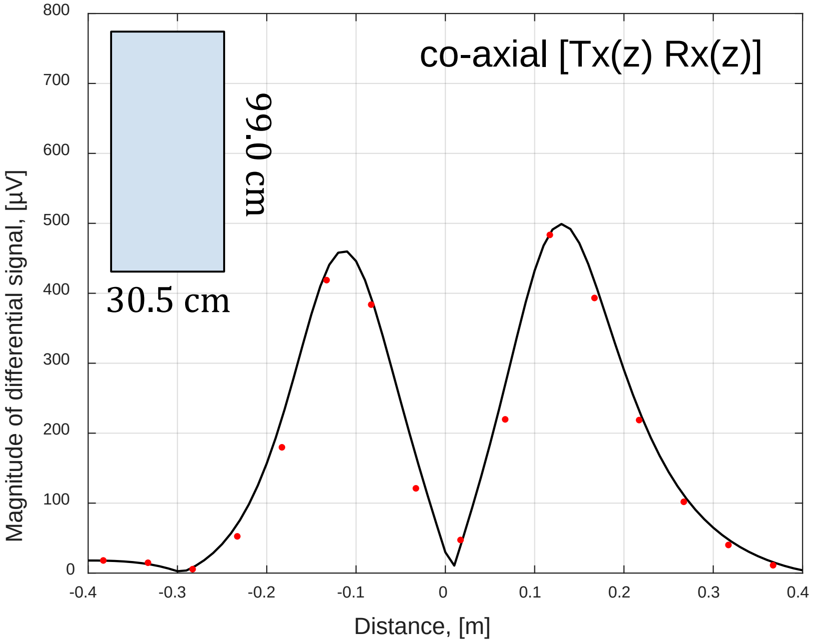

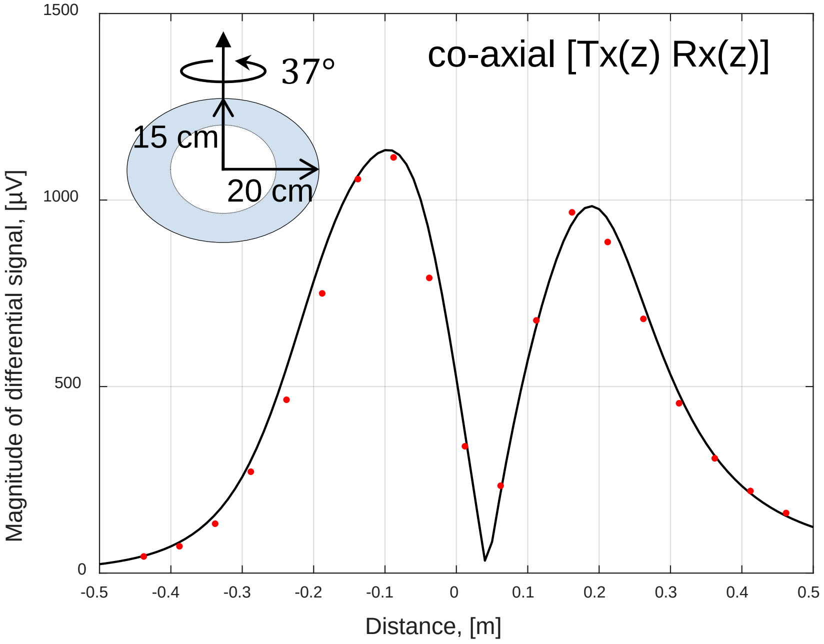

Development Plan

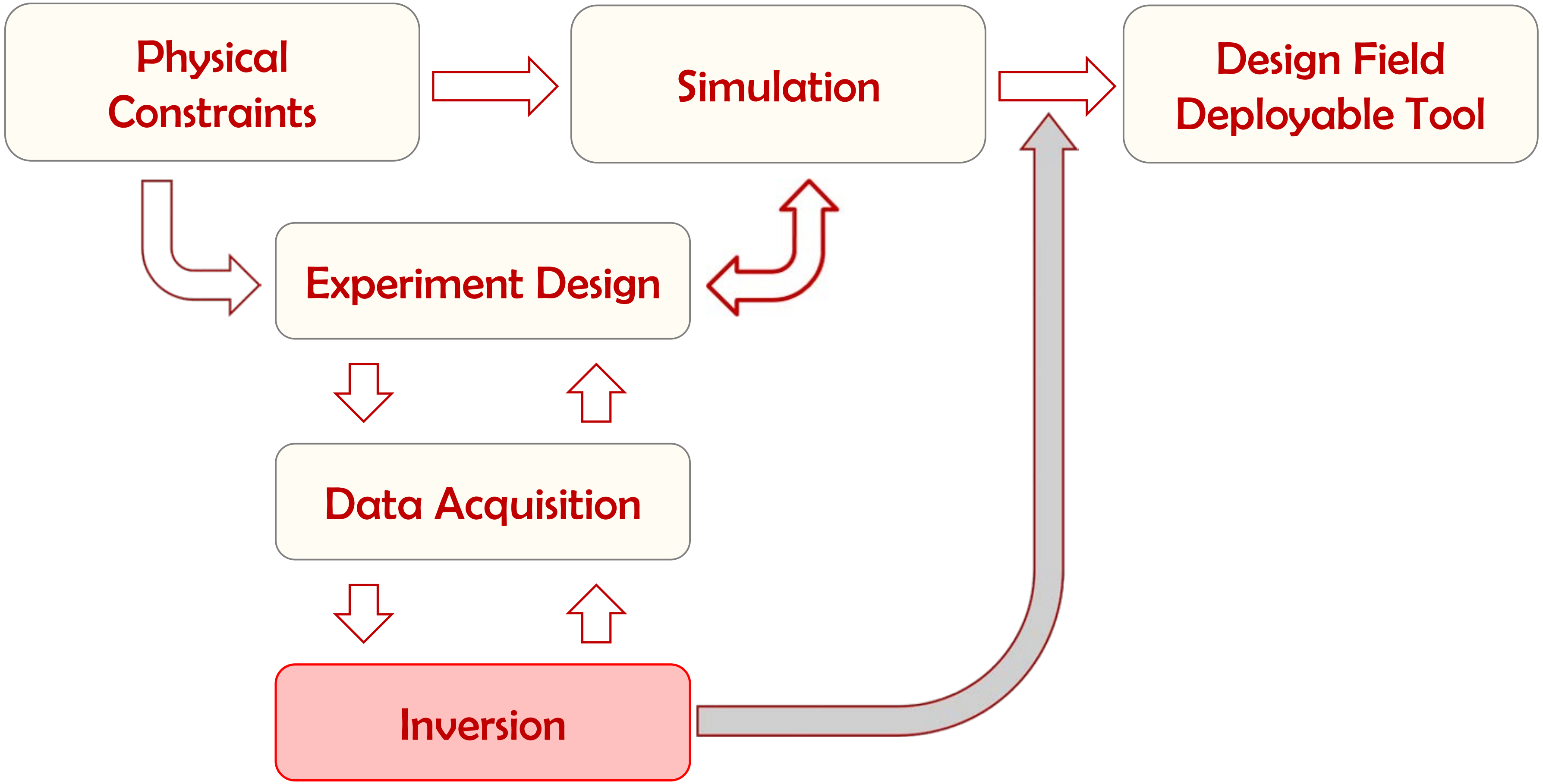

Tasks

- Task 1.0 -- Project Management Plan
- Task 2.0 - Development of forward model using proposed tool and different fracture geometries
- Task 3.0 - Lab testing of available proppants in the market for electrical and material properties
- Task 4.0 – Final design and construction of low frequency electromagnetic tool
- Task 5.0 – Laboratory and field testing of tool
- Task 6.0 -- Inverting the field data to obtain the fracture geometry

Inversion Strategy

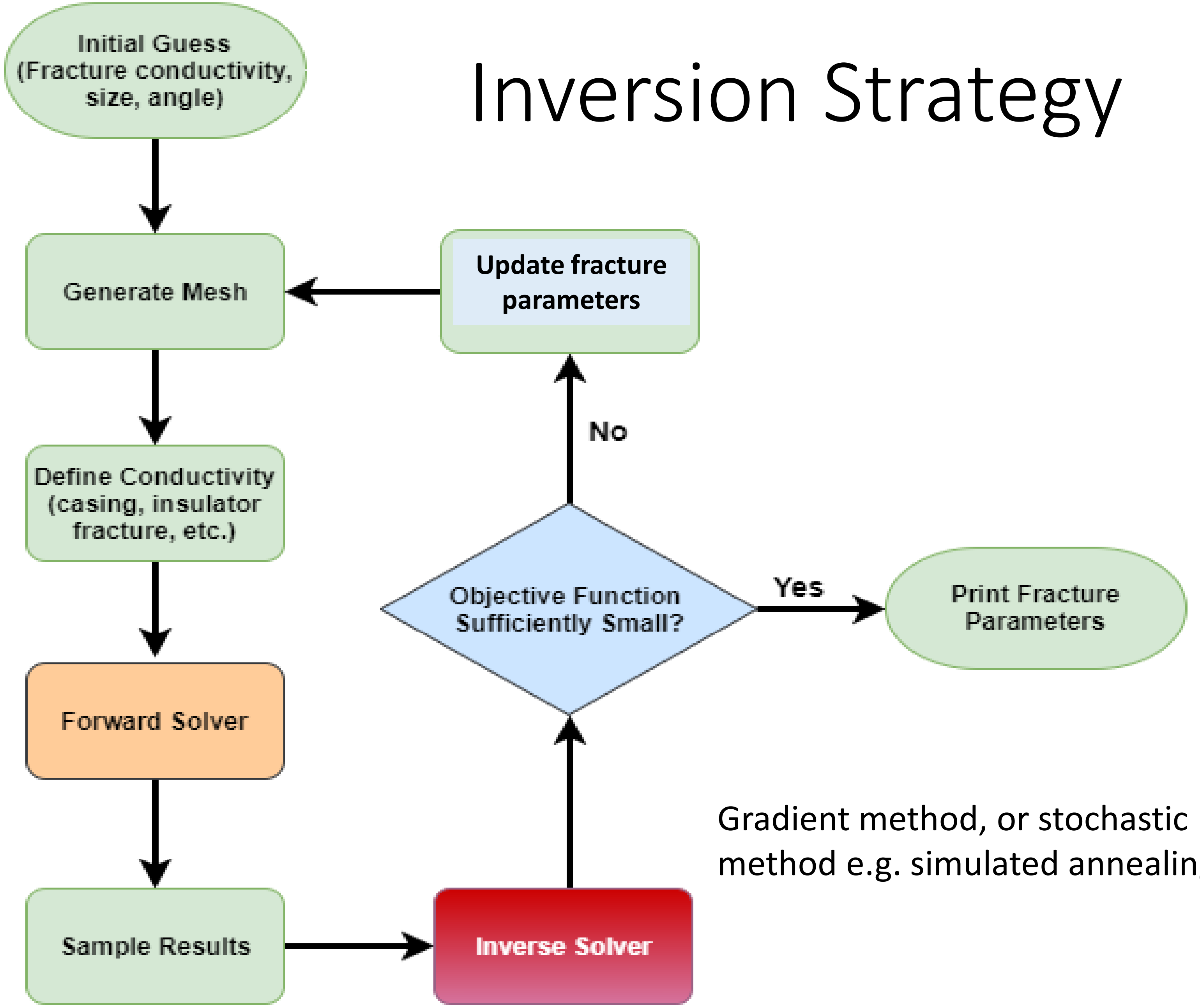

Gradient method, or stochastic method e.g. simulated annealing.

Example

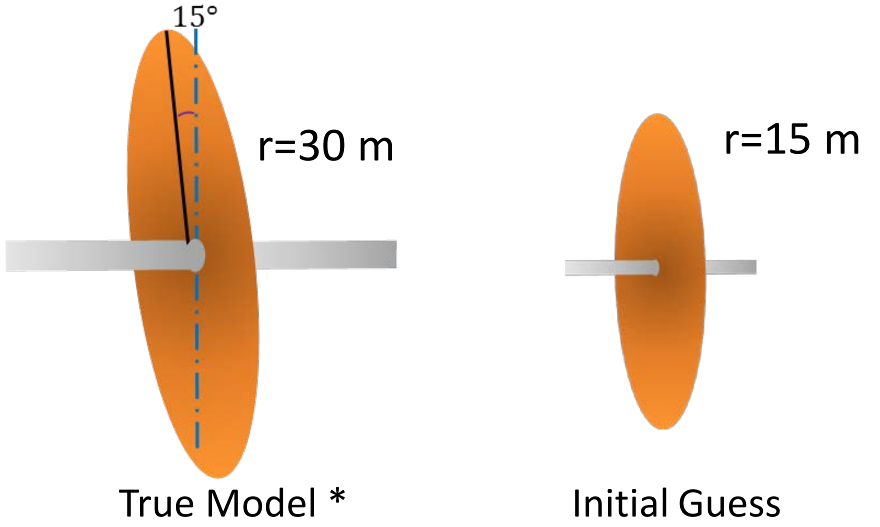

Objective Function $E(\bar{m}) = \|\Delta U - \Delta U_{true}\| = \sqrt{\sum_{i=1}^{n} [\Delta U_i(\bar{m}) - \Delta U_i(\bar{m}_{true})]^2}$

Voltage Difference $\Delta U_i = U_{frac,i} - U_{no-frac,i}$, i is the gap index

Model parameters $\bar{m} = [radius, angle]$

Inverse Problem

Gradient Descent + Backtracking Line Search

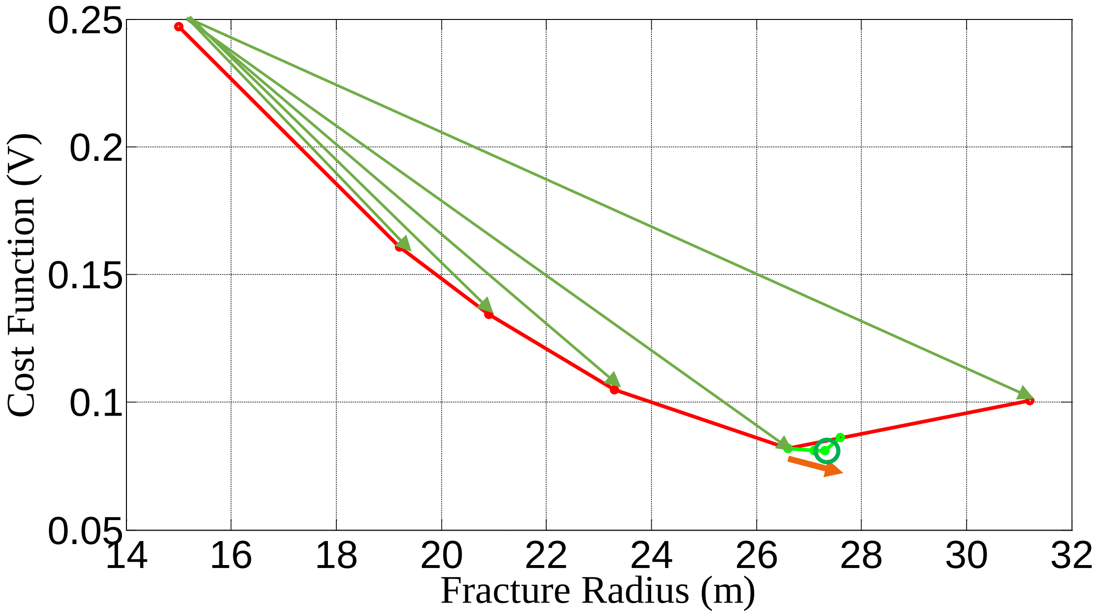

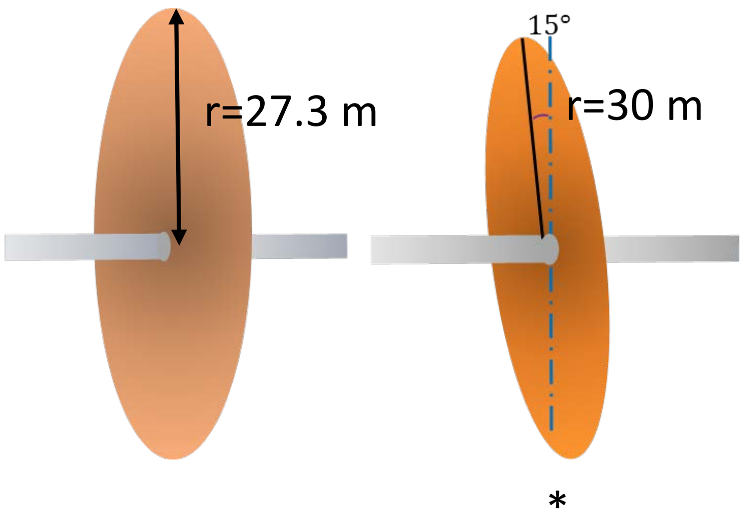

1. Calculate gradient g at starting point x_0
2. Move along direction in which the objective function decreases, for Δx (g), to $x_1 = x_0 + \Delta x$ (g)
3. If $E(x_1) < E(x_0)$, move forward for $1.4 \cdot \Delta x$, otherwise move forward for $0.8 \cdot \Delta x$, repeat until E increases
4. Go to step 1 until the gradient is small enough

Inverse Problem

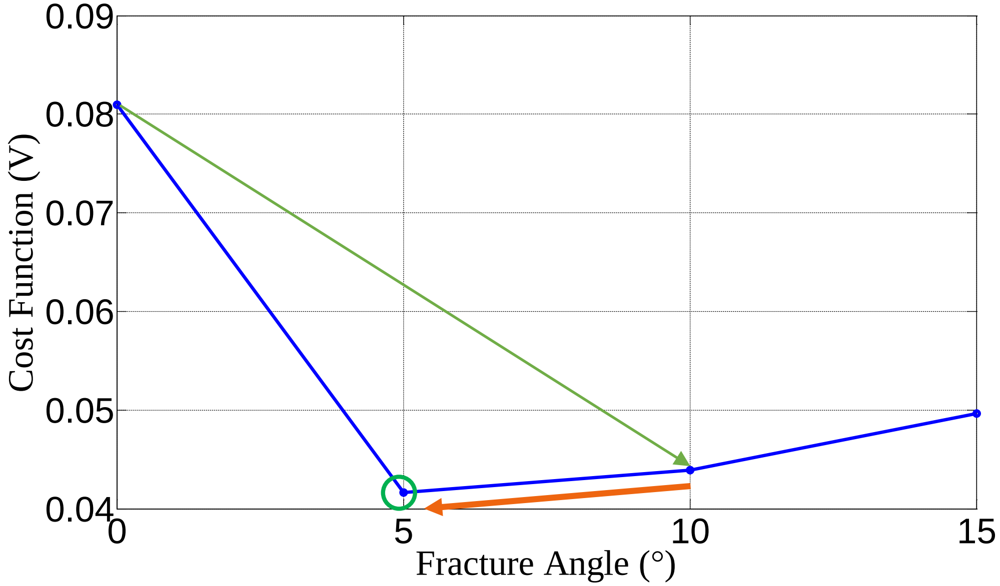

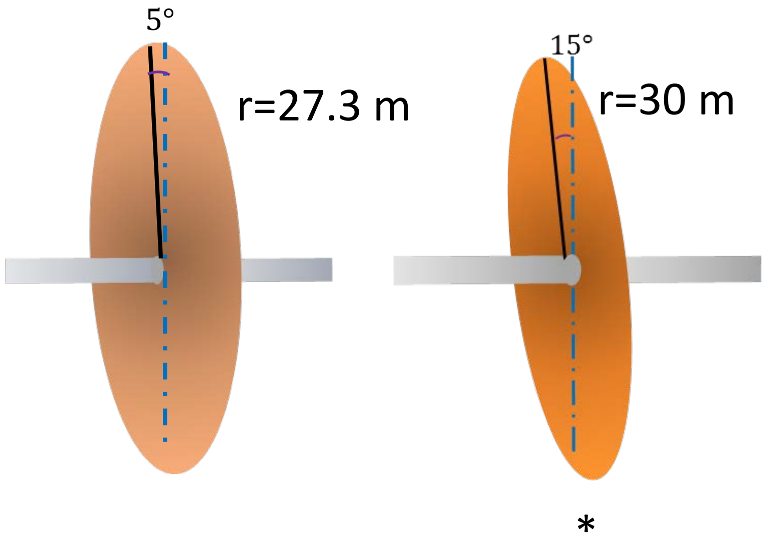

True Model
$r = 30\ m, \alpha = 15°$

VS

Estimated Model
$r = 27.3\ m, \alpha = 5°$

Current Status

Fully automatic inversion method being developed for the following fracture parameters: fracture length, height, conductivity and orientation.

Completed

- Parametric inversion of a single fracture from 'measured voltages' using gradient method and backtracking line search.

Being developed

- Simulated annealing inverse solver
- Inversion of multiple fractures with multiple excitation
- Incorporate simulated annealing inverse solver in the loop
- Using genetic algorithms to find a global minimum

Summary

- A lab prototype tool (transmitters and bucked receivers) has been built and tested in the lab and a shallow subsurface test site.
- Excellent agreement is obtained between the model predictions and the lab measurements for different T-R configurations.
- The results from the tests suggest that a commercial tri-axial EM tool can be built that has the potential to map the geometry of hydraulic fractures.
  - The prototype induction tool is shown to differentiate surface area, aspect ratio and dip angle of the fracture models used.
  - The highest signal levels occur when the primary magnetic field is perpendicular to the plane of the target.
  - From the principle of reciprocity, the response is the same if the source and receivers are interchanged.
  - Obtaining the same signal levels for a co-planar configuration is challenging because of wellbore constraints on transmitter coils.

E-Spectrum Technologies

The University of Texas at Austin
Petroleum and Geosystems Engineering

Thank you & Questions

Thanks to DOE for funding the project
DE-FE0024271

E-Spectrum Technologies

The University of Texas at Austin
Petroleum and Geosystems Engineering

Proppant: Experimental Results

Resistivity measurements for electrically conductive proppant

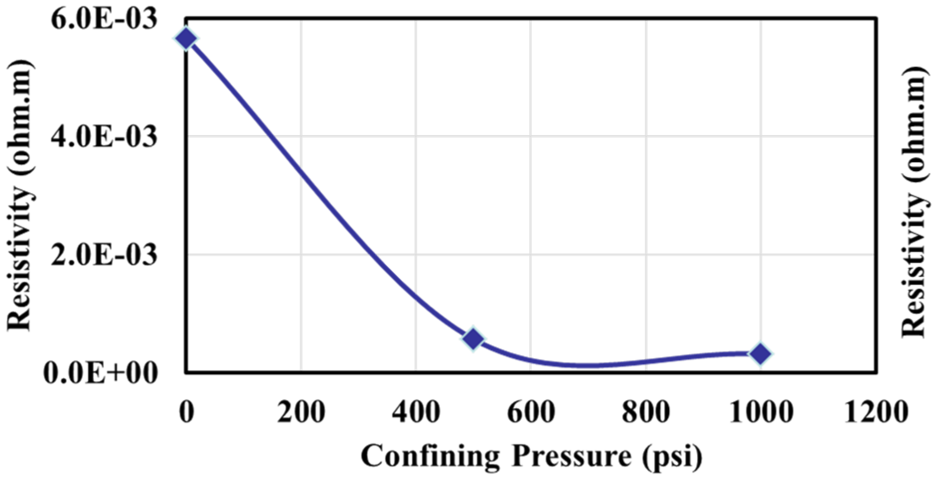

(a)

Density: 1.14 g/cm^3
Porosity: 43.9%
End point: 3.2x10^{-4} $\Omega \cdot m$

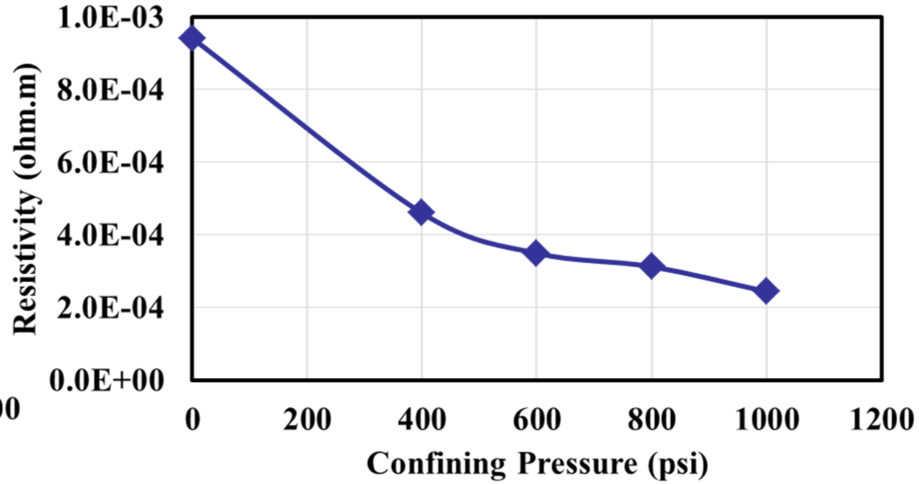

(b)

Density: 1.27 g/cm^3
Porosity: 37.6%
End point: 2.4x10^{-4} $\Omega \cdot m$

Fracture Conductivity and Normalized Conductivity for Sand and EC-Proppant

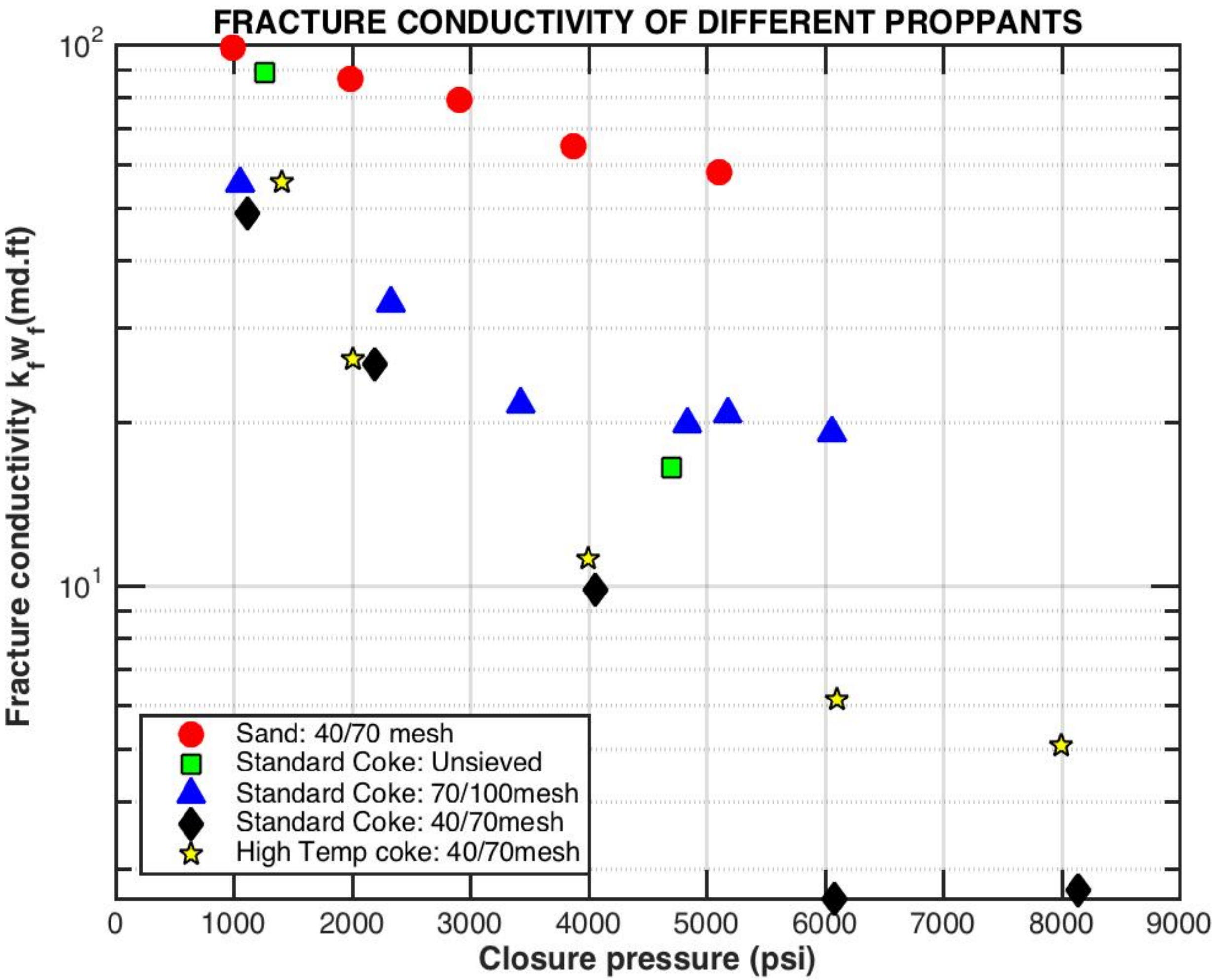

$F_{CD} = k_f * w / L_f * k$

$F_{CD} = 5 / (500*10^{-4})$

$F_{CD} = 100$

Normalized Conductivity for Sand and EC-Proppant

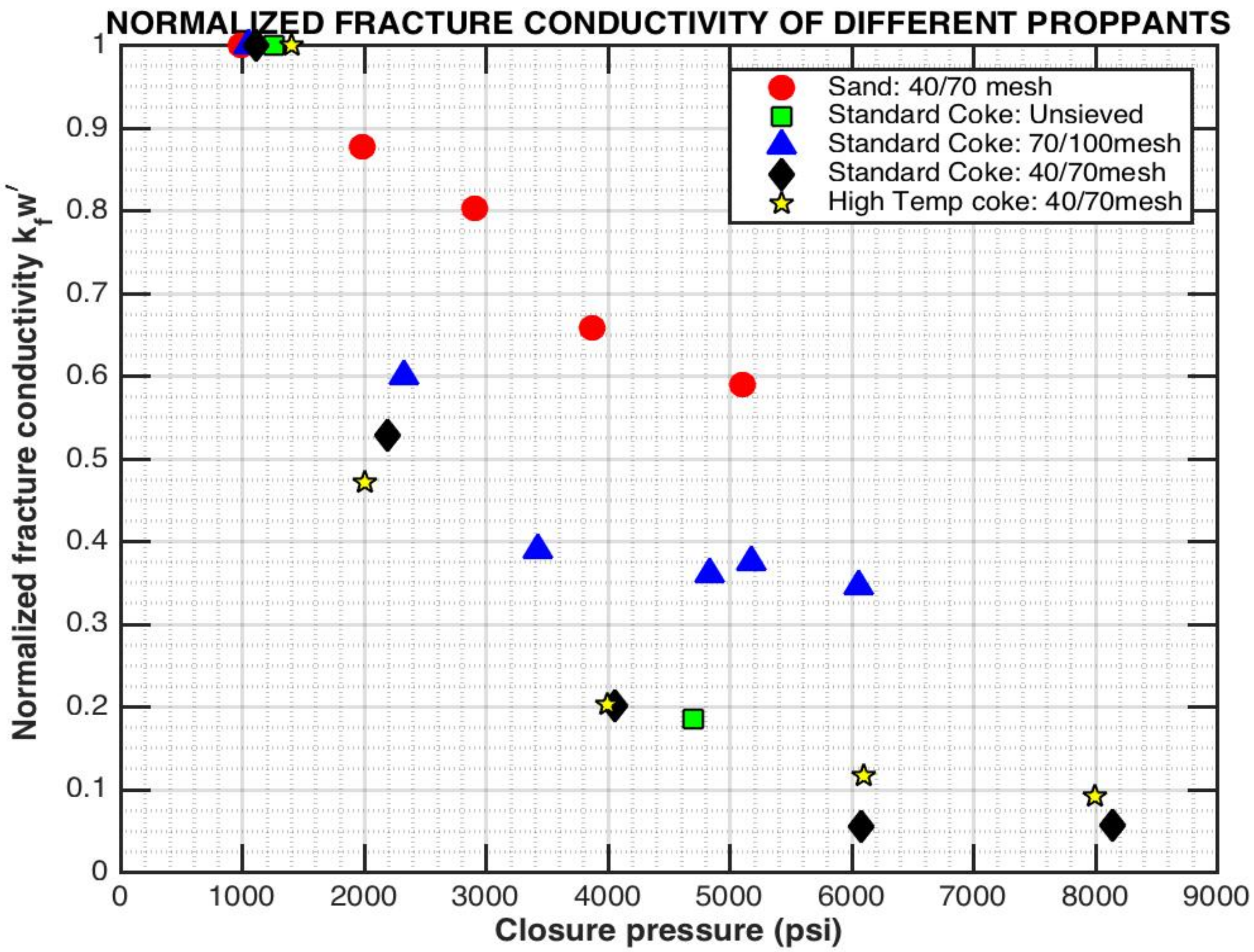

E-Spectrum Technologies

The University of Texas at Austin
Petroleum and Geosystems Engineering

Bucked Signal, Short Spacing, Fracture: 3m radius, 5mm thickness

Co-Axial (*zz*)

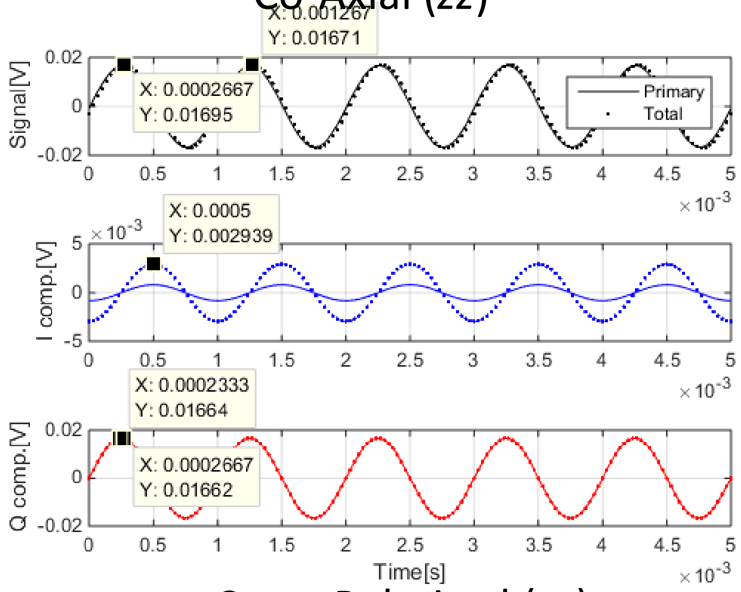

Co-Planar (*xx*)

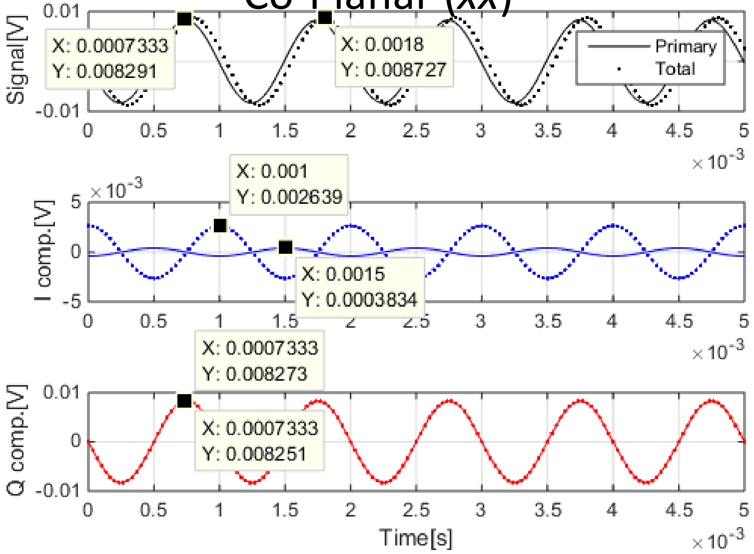

$$\sigma_{\text{frac}} = 333\ \text{S/m}$$
$$\sigma_{\text{bg}} = 0.333\ \text{S/m}$$

$$f = 1\ \text{kHz}$$
$$NI^{\text{peak}}A_{\text{TX}} = 150\ \text{Am}^2$$

$$N_{\text{RX}} = 1500\ \text{turns}$$
$$A_{\text{RX}} = 0.01\ \text{m}^2$$

Cross-Polarized (*xz*)

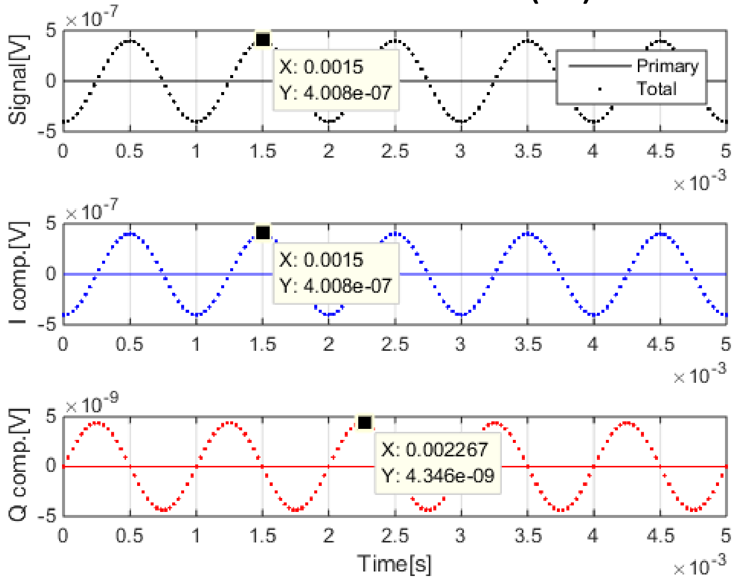

Cross-Polarized (*xy*)

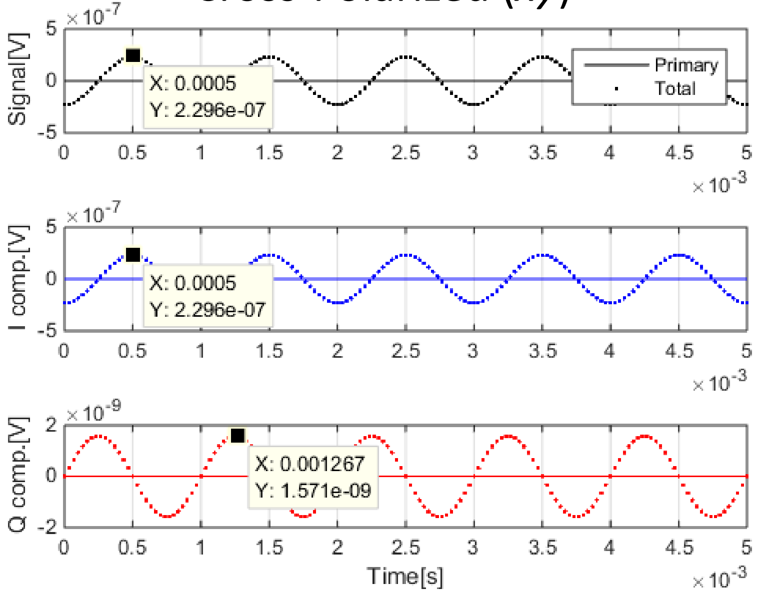

$$\Delta U = \frac{U_2}{n} - \frac{C_2}{C_1}U_1 n,$$

$n = 1.01$ – mismatch factor

$\frac{C_2}{C_1}$ – coefficient for perfect bucking

Extensive lab testing and simulations

The total signal comprises two contributions

- Primary signal: pre-fracing, response to formation only
- Secondary signal: change in signal due to fracture

$t_{\text{frac}} = 5$ mm
$r_{\text{frac}} = 3$ m
$\sigma_{\text{frac}} = 333$ S/m
$\sigma_{\text{bg}} = 0.333$ S/m

$f = 1$ kHz
$NI^{\text{peak}}A_{\text{TX}} = 150$ Am^2

$N_{\text{RX}} = 1500$ turns
$A_{\text{RX}} = 0.01$ m^2

Co-Axial (*zz*)

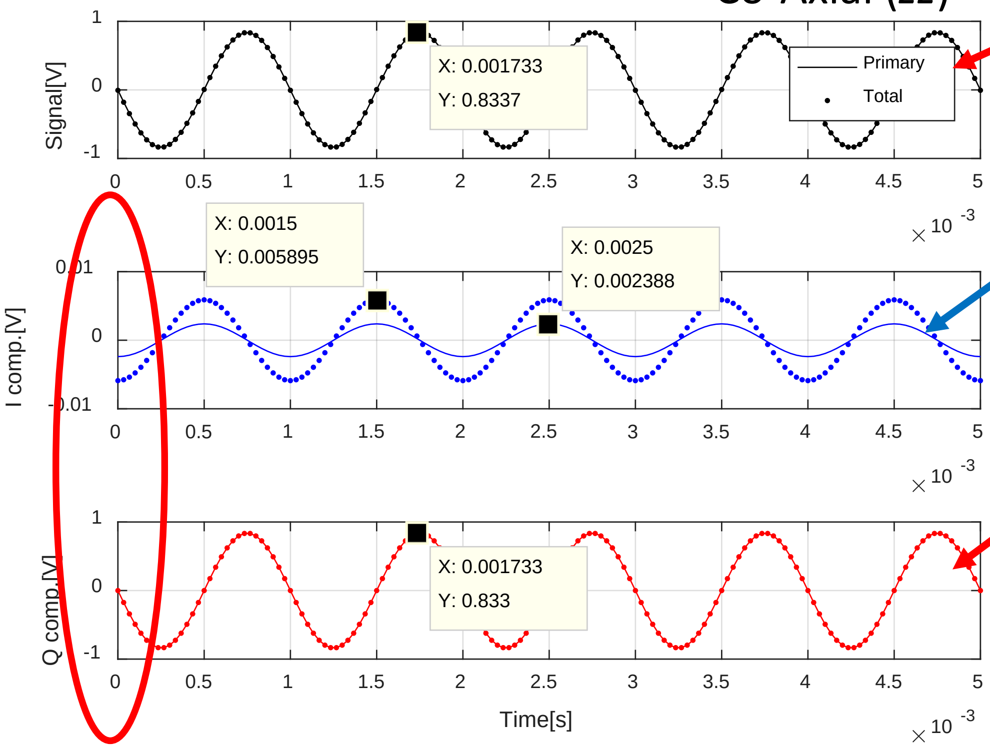

Primary signal dominates total

Fracture detectable in I-component

10% difference required in I-component to detect fracture

⇒10^4 dynamic range in total signal (without bucking)

⇒ 14 bit digital representation

Reason:

Quadrature(Q)-component overwhelms in-phase (I)-component

Fracture undetectable in Q component

E-Spectrum Technologies

The University of Texas at Austin
Petroleum and Geosystems Engineering

Comparison of Lab Results with Simulations

The total signal comprises two contributions

- Primary signal: pre-fracing, response to formation only
- Secondary signal: change is signal due to fracture

$$\Delta U = \frac{U_2}{n} - \frac{C_2}{C_1} U_1 n, \; U_{1,2} - \text{signals from two coils}$$

$$n = 1.01 - \text{mismatch factor}$$

$$\frac{C_2}{C_1} - \text{coefficient for perfect bucking}$$

$t_{\mathrm{frac}} = 5$ mm
$R_{\mathrm{frac}} = 3$ m
$\sigma_{\mathrm{frac}} = 333$ S/m
$\sigma_{\mathrm{bg}} = 0.333$ S/m

$f = 1$ kHz
$NI^{\mathrm{peak}} A_{\mathrm{TX}} = 150$ Am^2

$N_{\mathrm{RX}} = 1500$ turns
$A_{\mathrm{RX}} = 0.01$ m^2

Co-Axial (*zz*)

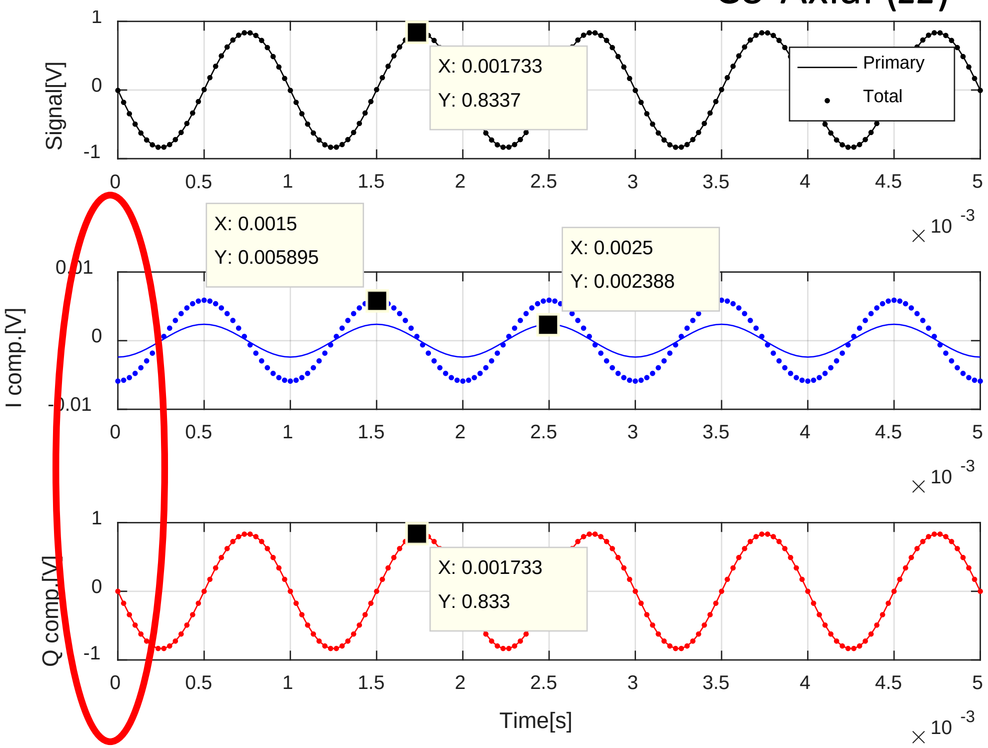

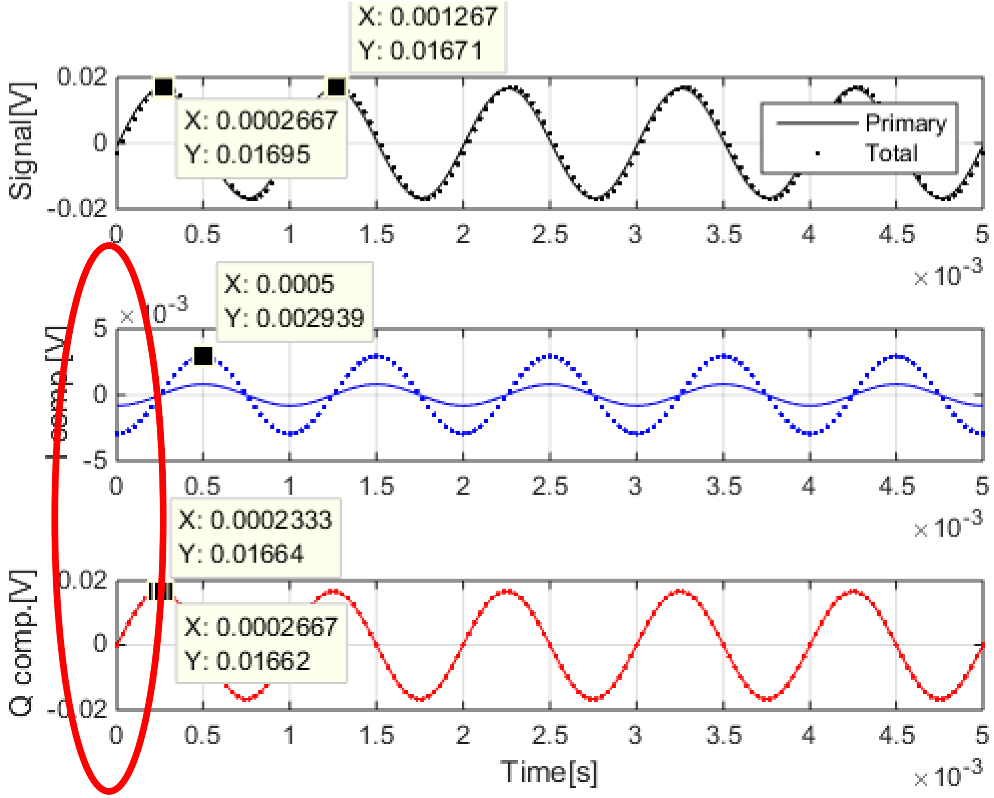

10% difference required in I-component to detect fracture

$\Rightarrow 10^{2\text{-}3}$ dynamic range in total signal (bucked)

$\Rightarrow$7-10 bit digital representation

Develop Commercial Tool Specifications (SBIR)

LFEI Tool Conceptual Design

- Consists of 7 sections assembled at wellhead
- First 3 sect. connect rigidly at fixed orientation
- Transmit Control Sub powered by monocable, controls electrical impulses sent to TX coils
- Transmit Coil Sub contains long-spacing TX coils and short/medium-spacing TX coils
- Short-Spacing Receiver Sub contains short-spacing bucking and RX coils, Dewar flask holding temperature-sensitive RX electronics, D&I package, RX batteries
- Medium- and Long-Spacing Receiver Subs similar to short-spacing receiver sub
- Medium Wired Spacer Bar spaces receiver sub so that medium-spacing RX coils are 20 ft away from *z* TX coil
- Long Wired Spacer Bars (3 ea) space receiver sub so that long-spacing RX coils are 60 ft away from the *z* TX coil
- Tool Wiring Bus extends through each spacer bar and allows communication between Transmitter Control Sub and each receiver sub

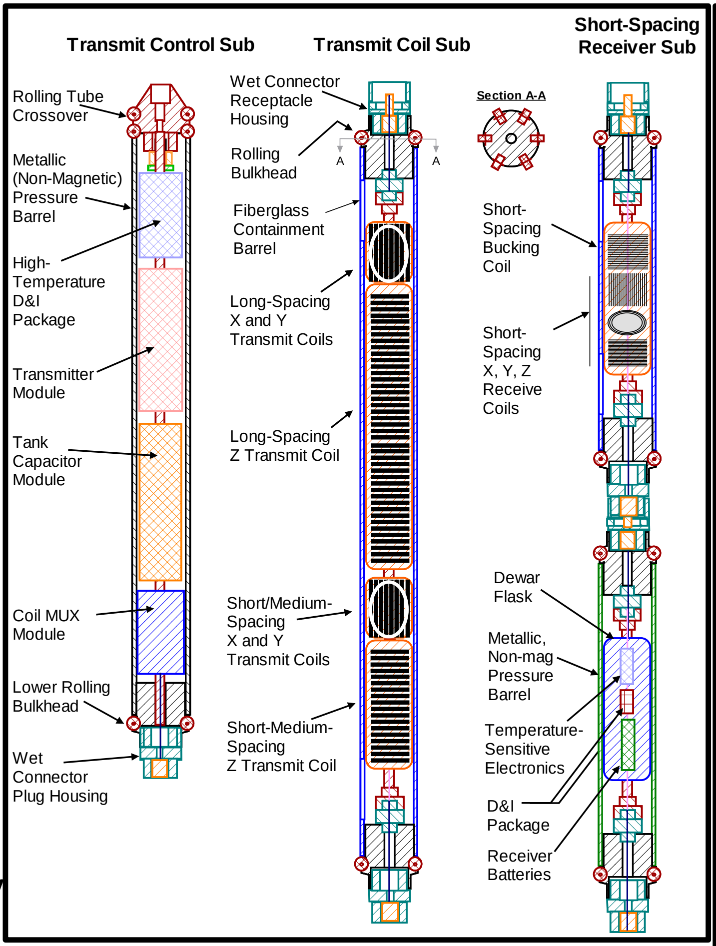

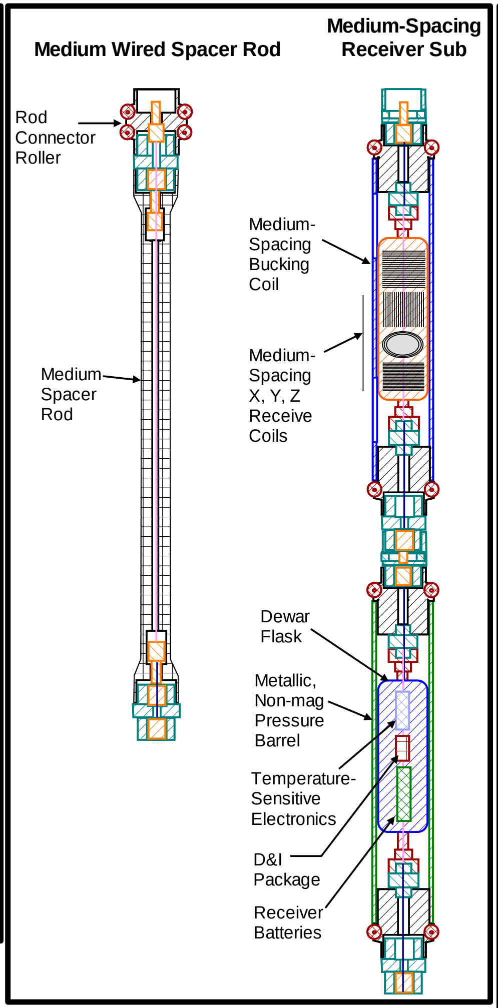

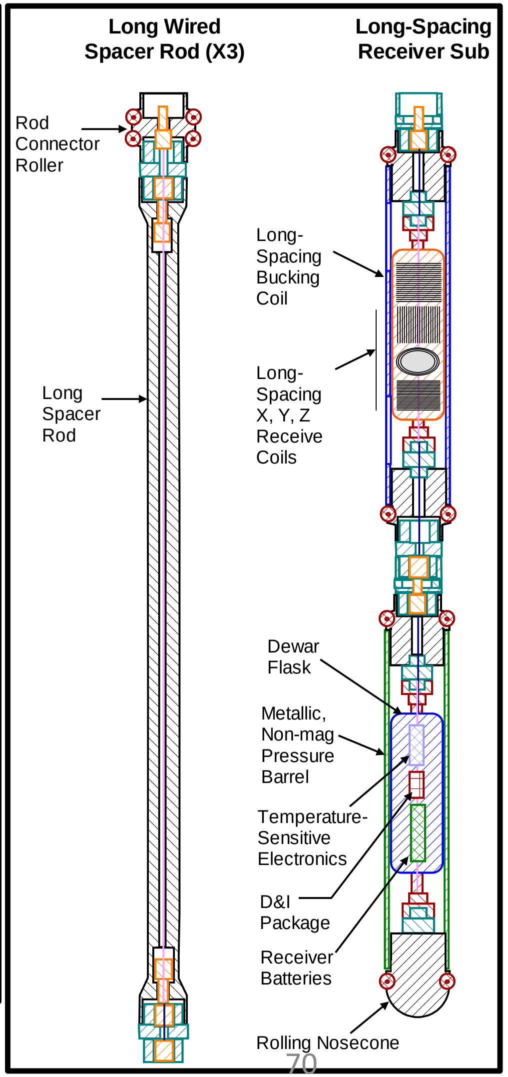

- Rolling Bulkheads on end of each sub reducing sliding friction against tool in horizontal wellbores

Response Function Space

- The best response of EM tool occurs when the primary magnetic field is perpendicular to the plane of the target; it was also shown in the previous experimental study:

Parameter	**Co-Axial**	**Co-Planar**	**Cross-Polarized**
Surface Area	**>100 µV**	>10 µV	<1 µV
Aspect Ratio	**>100 µV**	>10 µV	<1 µV
Dip Angle	**>100 µV**	>100 µV	**>100 µV**

- The main motivation of the inversion analysis is to provide the same level of parameter accuracy (when compared to tri-axial coil system) when only coil couples with the strongest signals are used.

2) Directly Solving for the Conductivity

Error minimization (L_2 norm)

$$f(G) = \sum_i \left(V_i^{\text{sca}} - \tilde{V}_i\right)^2$$

$$\downarrow$$

$$\frac{\partial f}{\partial G} = 0$$

$$\downarrow$$

$$\sum_i V_i^{\text{sca}} \frac{\partial V_i^{\text{sca}}}{\partial G} = \sum_i \tilde{V}_i \frac{\partial V_i^{\text{sca}}}{\partial G}$$

Simplification to the forward algorithm

$$\mathbf{V}_i^{\text{sca}} = -j\omega\mu_{\text{o}} N_{\text{rx}} A_{\text{rx}} \underline{\mathbf{K}}_i^{\text{T}} \left[\underline{\underline{\mathbf{B}}} \backslash \underline{\mathbf{V}}_i^{\text{inc}}\right] G$$

$$V_i^{\text{sca}} = G T_i \qquad \frac{\partial V_i^{\text{sca}}}{\partial G} = T_i$$

$$T_i = -j\omega\mu_{\text{o}} N_{\text{rx}} A_{\text{rx}} \underline{\mathbf{K}}_i^{\text{T}} \left[\underline{\underline{\mathbf{B}}} \backslash \underline{\mathbf{V}}_i^{\text{inc}}\right]$$

$$\boxed{G = \left[\underline{\mathbf{T}}^{\text{T}} \underline{\tilde{\mathbf{V}}}\right] / \left[\underline{\mathbf{T}}^{\text{T}} \underline{\mathbf{T}}\right]}$$

$$\uparrow$$

Given the measured voltage, tool parameters and assumed fracture shape, what is the conductivity?

Orthogonal Fractures

Case 1: Circular fracture with uniform conductivity

- Radius is 4m; orthogonal and planar fracture
- Conductance is uniform and equal to 0.1 S; thickness is 1 mm and conductivity is 100 S/m.

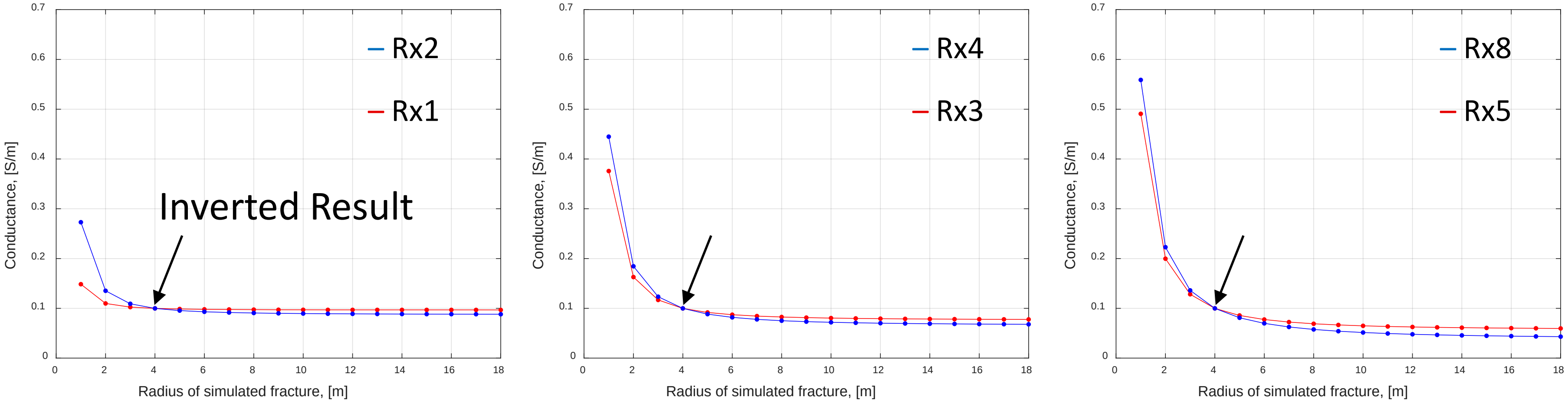

Inverted data perfectly matches input values for the different transmitter-receiver spacing.

Electromagnetic Scattering

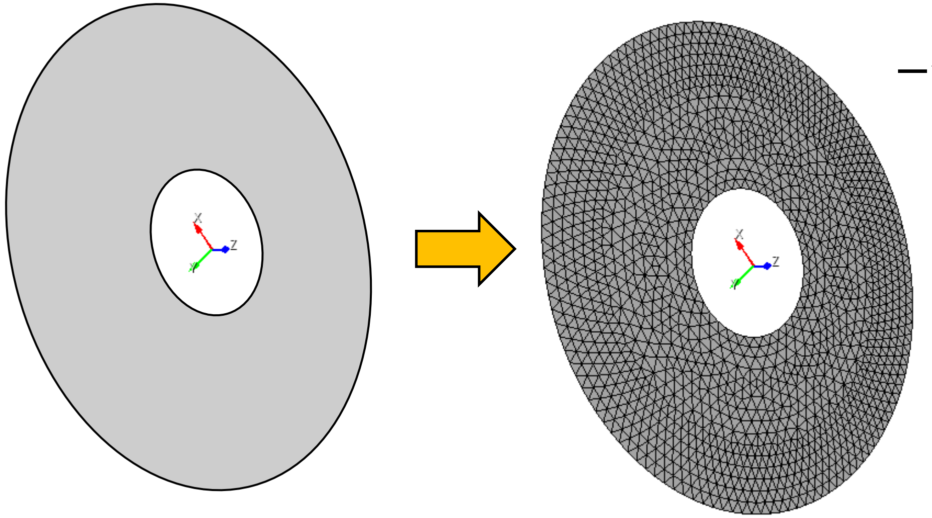

$$-\hat{n}\times\hat{n}\times\mathbf{E}^{\mathrm{sca}}-\frac{\mathbf{J}}{\sigma t}=\hat{n}\times\hat{n}\times\mathbf{E}^{\mathrm{inc}}(\mathbf{r})\quad \mathbf{r}\in S$$

and $$\mathbf{J}(\mathbf{r})\cong\sum_{n=1}^{N} I_n\boldsymbol{\Lambda}_n(\mathbf{r})$$

$$\mathbf{Z}\mathbf{I}=\mathbf{V}^{\mathrm{inc}}$$

- Once unknown coefficient vector is found, scattered fields are calculated for two observation points.
- This procedure is repeated for each tool position and only incident field vector is regenerated.